



# Review on the diffusive and interfacial performance of bituminous materials: From a perspective of molecular dynamics simulation



Shisong Ren<sup>\*</sup>, Xueyan Liu, Peng Lin, Yangming Gao, Sandra Erkens

Section of Pavement Engineering, Faculty of Civil Engineering & Geosciences, Delft University of Technology, Delft, Netherlands

## ARTICLE INFO

### Article history:

Received 30 June 2022

Revised 2 September 2022

Accepted 10 September 2022

Available online 16 September 2022

### Keywords:

Sustainable bituminous materials

Molecular dynamics simulation

Dynamic diffusion behavior

Self-healing mechanism

Interfacial bonding performance

## ABSTRACT

The cohesive and adhesive performances of bituminous materials significantly affect the service life of asphalt pavement. The molecular dynamics (MD) simulation method has been proved as an effective tool to predict the thermodynamics parameters of different multi-substance and multi-phase bitumen models during different diffusion, self-healing, and interfacial interaction processes. This paper aims to comprehensively review the application cases of MD simulations on dynamic and interfacial bitumen systems. The diffusion behaviors of oxygen, moisture, and rejuvenator molecules in the bitumen matrix could be illustrated from MD simulations considering the influence of temperature, pressure, and humidity. Moreover, molecular mobility and distribution of bitumen molecules on the aggregate surface remarkably influenced the interfacial bonding level and moisture sensitivity. In addition, the molecular-scale mechanism and evaluation indices for the self-healing potential of bitumen models were reviewed. Further, the representative bitumen-(moisture)-aggregate interfacial models, the corresponding evaluation parameters, and influence factors for the adhesive bonding strength in MD simulations were overviewed. Besides, the effects of bitumen components, aggregate type, moisture invasion, temperature variation, and pull-off tension rate on the adhesion performance of bitumen-aggregate models were summarized and discussed. This review can help us fundamentally understand the dynamic diffusion, self-healing behaviors, and interfacial characteristics of bitumen models at the atomic level and develop more potential functions of MD simulations in addressing the scientific issues of sustainable bituminous materials.

© 2022 The Author(s). Published by Elsevier B.V. This is an open access article under the CC BY license (<http://creativecommons.org/licenses/by/4.0/>).

## Contents

1. Introduction	2
2. Review route and structure	4
3. Application fields of MD simulations	4
4. Applications of MD simulations in dynamic systems of bitumen	5
4.1. Diffusion behaviors of external substances and bitumen molecules	6
4.1.1. The diffusion of oxygen and moisture in bitumen	6
4.1.2. The diffusion of rejuvenator in aged bitumen	8
4.1.3. The diffusion of bitumen components on the aggregate surface	9
5. Self-healing characters of bituminous materials	9
5.1. Self-healing phenomenon and potential mechanism	9
5.2. Molecular-scale self-healing models	9
5.3. Multiscale evaluation on self-healing performance	10
5.4. Influence factors on self-healing behavior	11
6. Applications of MD simulations in interfacial bituminous systems	13
6.1. Basic knowledge	15
6.1.1. Interfacial molecular models	15

<sup>\*</sup> Corresponding author.

E-mail address: [Shisong.Ren@tudelft.nl](mailto:Shisong.Ren@tudelft.nl) (S. Ren).

6.1.2.	Influence factors . . . . .	15
6.1.3.	Evaluation parameters . . . . .	16
6.2.	Materials factors on adhesion bonding of interfacial systems . . . . .	16
6.2.1.	Aggregate characteristics . . . . .	16
6.2.2.	Bitumen performance. . . . .	19
6.3.	External factors for adhesion bonding of interfacial systems. . . . .	20
6.3.1.	Moisture invasion. . . . .	20
6.3.2.	Temperature variation . . . . .	21
6.3.3.	Pull-off loading rate . . . . .	21
7.	Conclusions and recommendations. . . . .	22
7.1.	Main conclusions. . . . .	23
7.2.	Recommendations for future works. . . . .	23
	CRediT authorship contribution statement . . . . .	23
	Declaration of Competing Interest . . . . .	23
	Acknowledgments . . . . .	23
	References . . . . .	23

## 1. Introduction

The design and construction of sustainable asphalt roads is a common purpose of pavement researchers and engineers, and it is necessary to exhibit satisfactory cohesive and adhesive performance [1]. However, this target is meaningful but challenging because of the complicated environmental and material factors [2]. It is inevitable for the bitumen to go through the aging process under complex air pressure, temperature, and humidity conditions [3]. The cohesion and adhesion properties of the asphalt mixture deteriorated remarkably as the increment in the aging degree of binder [4]. Fortunately, the self-healing characteristic of bitumen would restore the cohesive bonding and weaken its crack level to some extent [5]. On the other hand, it is expected that incorporating a rejuvenator can restore the cracking resistance, interfacial bonding strength, and moisture resistance of recycled asphalt materials [6,7].

It is easy to notice that there are lots of multi-substance and multi-phase systems of asphalt materials during different aging [8], self-healing [9], and rejuvenation procedures [10], which arouses research topics on the thermodynamic diffusion of one substance to another matrix [11] and the binding strength

between different phases [12]. Fig. 1. illustrates the main diffusive and interfacial issues in bituminous materials, which are attributed to the sustainability of asphalt pavement [13]. The asphalt mixture comprises bitumen binder and aggregate, and the interaction strength between bitumen and aggregate phases determined the adhesion performance of the asphalt mixture [14,15]. Moreover, the interaction of the bitumen-moisture-aggregate three-phase system were remarkably related to the moisture damage level to the mechanical properties of the asphalt mixture [16]. In addition, the diffusion capacity and chemical component distribution of bitumen on the aggregate surface played a crucial role in the adhesion performance of the asphalt mixture [17].

The diffusive behaviors of oxygen, moisture, and rejuvenators in bitumen matrix are research hotspots for developing a sustainable asphalt pavement with adequate resistance to oxidative aging and moisture damage [18]. The oxygen and moisture concentrations affecting the aging level of bitumen were associated with the diffusion rate [19]. Meanwhile, it has been proved that rejuvenators' diffusion capacity greatly influenced the blending and homogeneity levels of rejuvenated bitumen [20]. Heterogeneous distribution of rejuvenators in aged bitumen would result in rutting and cracking distresses [21]. Furthermore, it was reported that the underly-

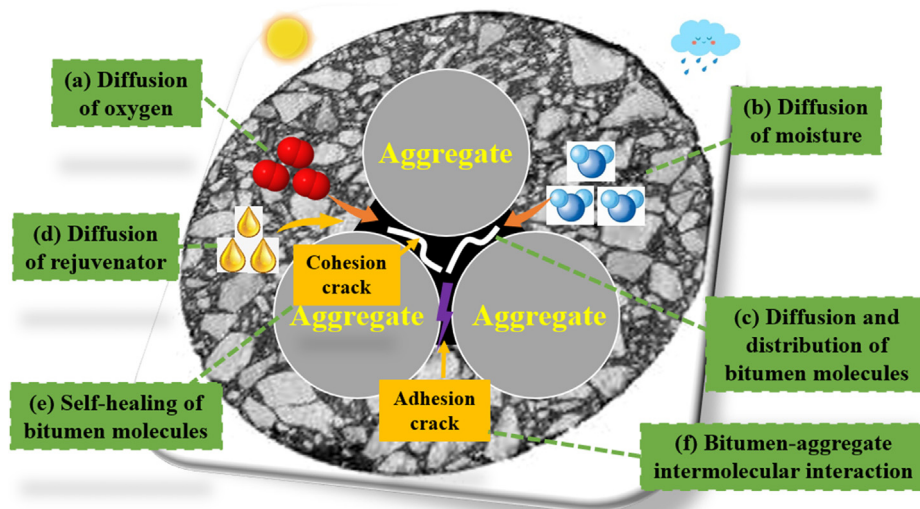


Fig. 1. The research topics on multi-substance and multi-phase systems of asphalt materials.

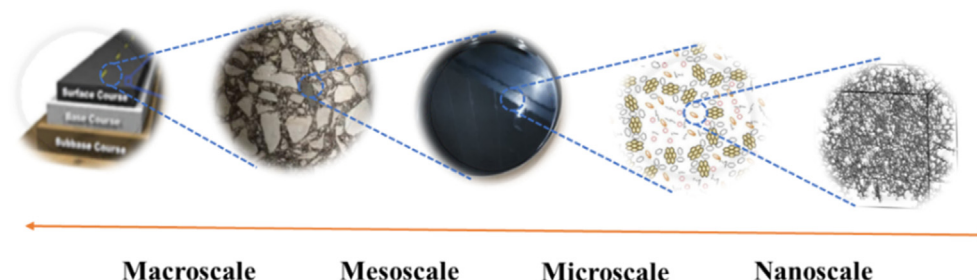


Fig. 2. Multiscale evaluation method of bituminous materials [46].

ing mechanism of self-healing characteristic of bitumen was mainly composed of molecular diffusion, micro-crack disappearance, intermolecular interaction, and cohesion strength recovery [22,23].

The transport and interfacial properties were important to develop sustainable bituminous materials [24], and different experimental characterization methods have been proposed to qualitatively and quantitatively evaluate the diffusion and adhesion parameters. The pressure decay method, electrodynamic balance, and chemo-mechanical characterizations with a diffusion-reaction equation were utilized to measure the diffusion coefficient of oxygen in bitumen and mastic [25–28]. Meanwhile, the experimental methods of FTIR-MIR, gravimetric test, and dynamic vapor sorption are always conducted to determine the diffusion coefficient parameters of moisture in different bituminous materials [29–31]. Due to the high vaporization points of liquid rejuvenators and considerable blending potential with bitumen, it is challenging to perform the pressure decay method, gravimetric test, and dynamic vapor sorption for measuring their diffusion rate in aged bitumen [32]. Therefore, the diffusion coefficient values of rejuvenators are always obtained through carrying out a two-layer diffusion test together with chemical (ATR-FTIR), rheological (DSR), and morphology (AFM and nanoindentation test) characterizations [33–35]. Moreover, the solvent extraction method was a common way to distinguish the concentration difference distribution of rejuvenators in aged bitumen when the diffusion process took place in the asphalt mixture [36].

Concerning the evaluation methods of the adhesion property between bitumen binder and aggregate, numerous physical, mechanical, and chemical tests have been proposed, including the pull-off tension test [37], peel test [38], boiling method [39], net-adsorption test [40], contact angle method [41], surface free energy [42], and atomic force microscopy (AFM) [43]. Different mechanical and thermodynamic parameters were utilized to assess the interfacial bonding strength between bitumen and aggregate [44]. Although these macroscale characterization methods could measure the diffusion rate of oxygen, moisture, and rejuvenator in bituminous materials, and the self-healing ratio of bitumen under different temperatures and rest period conditions,

they still showed several shortcomings [45]. For instance, (i) The experimental results were remarkably dependent on the type of evaluation method; (ii) Most of these tests were complicated and time-consuming; (iii) The human error showed a non-negligible influence on the final results. (iv) It was difficult to explain the transport mechanism and interfacial characteristics between the bitumen fractions with oxygen, moisture, rejuvenator, and aggregate; (v) Some essential thermodynamics and atomic-level structural parameters were unavailable from macroscale experimental tests.

To this end, a multi-scale evaluation method (shown in Fig. 2) of bituminous materials is recommended to fundamentally understand the interaction mechanism of the different physical and chemical phenomena of bituminous materials at the atomic scale and develop more efficient and sustainable pavement materials from a start point of molecular design and optimization [47]. The diffusion coefficient values of oxygen, moisture, and rejuvenator molecules in bitumen models could be predicted from MD simulations, which were consistent with experimental results [48]. Meanwhile, the dynamic diffusion behaviors of these molecules in the bitumen matrix could be visualized, and the intermolecular interaction between various bitumen molecules with the oxygen, moisture, and rejuvenator molecules could be quantified. Thus, it is beneficial to optimizing the molecular components of bitumen with sufficient resistance to oxidative aging and moisture damage, and designing more efficient rejuvenator molecules with strong molecular mobility. In addition, the diffusion behaviors and molecular distributions of different SARA fractions in bitumen on the aggregate surface could be outputted and distinguished from MD simulations, which was hardly achieved from conventional experiments [49].

The self-healing mechanism at a molecular scale of bituminous materials has been investigated and explored using MD simulations under the different conditions of bitumen components, temperature, and healing agent [50]. The molecular mobility of SARA fractions in bitumen during a self-healing procedure could be calculated and compared [51]. Meanwhile, the influence of aging, modification, and rejuvenation on the self-healing rate and ratio of bitumen have also been studied in MD simulations [52]. For a

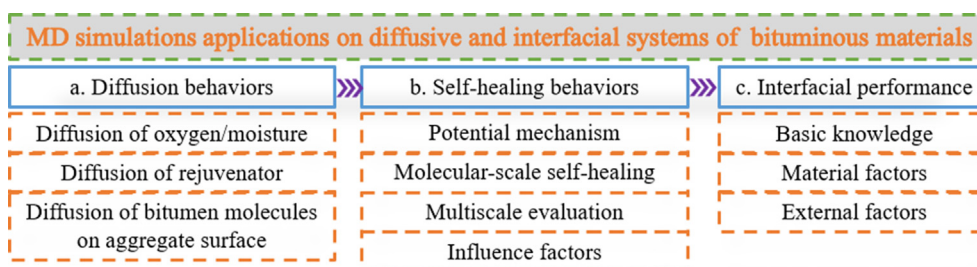


Fig. 3. The review route and structure.

bitumen-aggregate interface, the MD simulations have been employed to predict the interfacial bonding strength, debonding potential, and molecular-level destruction form under a condition of tension force [53]. Notably, the effects of different material characteristics (bitumen and aggregate component) and external factors (temperature, moisture, and pull-off) on the adhesion performance have been considered during the MD simulations on the bitumen-aggregate interface models [54].

Nowadays, the MD simulation method is widely employed in multi-substance and multi-phase systems of bituminous materials to calculate the diffusion coefficient parameters of oxygen, moisture, and rejuvenator molecules in bitumen models, as well as to assess the interfacial bonding performance and moisture damage resistance of bitumen-aggregate systems. However, limited review work has been conducted to summarize the application cases of MD simulations in investigating the transport and interfacial performance of different multi-substance and multi-phase systems of bituminous materials. It is impossible to review all research points on bitumen and asphalt materials. This review will focus on the application cases of MD simulations on most diffusion and interface models of bituminous materials at the molecular level. It should be mentioned that diffusion behavior and interfacial interaction between different substances and phases are physical processes with no chemical reaction. First, we will focus on the transport characteristics of oxygen, moisture, and rejuvenator molecules in the bitumen model, as well as the molecular mobility and distribution of bitumen components on the aggregate surface. Afterward, the previous literatures of MD simulation to evaluate the self-healing capacity of bitumen and explain the self-healing mechanism at an atomic level will be summarized. Lastly, the utilization of MD simulations on the bitumen-aggregate interface models related to the adhesion crack potential of the asphalt mixture will be reviewed.

## 2. Review route and structure

Fig. 3 illustrates the review route and structure mainly on the application cases of MD simulations on both dynamic and interfacial systems of bituminous materials. Firstly, the MD simulations on investigating the diffusion behaviors of oxygen and moisture molecules in bitumen models are reviewed, which significantly promotes the oxidative aging and moisture damage of bituminous materials. Afterward, the MD simulation cases in dynamic migration capacity evaluation of various rejuvenator molecules in aged

bitumen are introduced. Moreover, the difference in molecular mobility and distribution between different bitumen molecules on the aggregate surface could be observed and estimated with MD simulations. In addition, the MD simulation studies on self-healing performance assessment and mechanism explanation of bituminous materials are overviewed, considering the influence of temperature, crack width, and healing agent.

On the other hand, the MD simulation studies on characterizing the adhesion bonding and moisture damage resistance of the bitumen-aggregate interface are reviewed. The representative molecular models of bitumen-(moisture)-aggregate interfacial systems and the corresponding evaluation parameters for the adhesion bonding level and moisture susceptibility predicted from MD simulations are summarized. Furthermore, the influence of the material characteristics (bitumen and aggregate components) and external factors (temperature, moisture, and pull-off loading rate) on the interfacial bonding strength of bitumen-aggregate models are generalized.

## 3. Application fields of MD simulations

In light of its irreplaceable effects, the MD simulation method is employed in different fields of food [55], medicine [56], energy and fuels [57], chemistry [58], and polymer [59]. Moreover, as shown in Fig. 4, the MD simulation method is vital in multiscale studies in multidisciplinary materials engineering, chemical engineering, and physical and applied physics. In this review, the application fields of MD simulation will be introduced with the classification of the study perspective, including mass transition, mechanical response, reaction mechanism, and interfacial interaction. Although the MD simulation method involves all aspects, these four points are extensively researched in bituminous materials and thus discussed herein.

- **Mass transition:** The mass, energy, and momentum transitions are common and ubiquitous in our lives and studies. Through the MD simulation, the mass transition process could be observed visually at an atomic level.
- **Mechanical response:** The mechanical response is the inner structure change of materials under external force. The MD method can be employed to simulate the intermolecular interactions between different substances and reflect the mechanical response, which is the principle of the atomic force microscope.

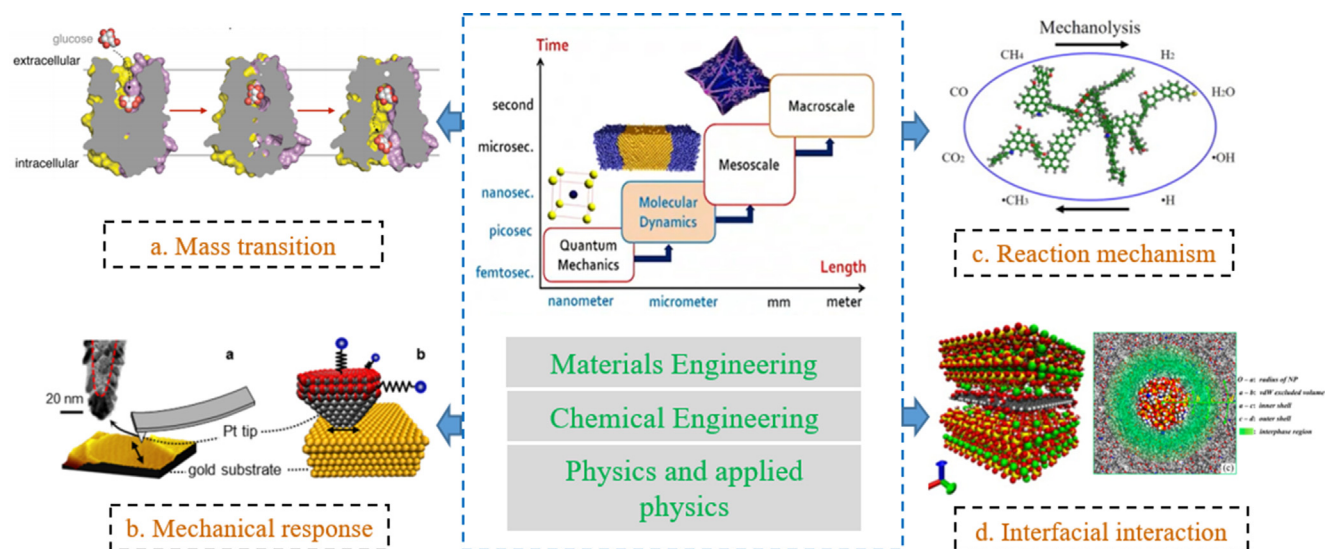


Fig. 4. The application fields of MD simulation.



- **Reaction mechanism:** The molecular interaction and reaction mechanism can be explored with MD simulations. Meanwhile, the transition state of matters during chemical reactions is easily captured, which is beneficial to understanding the reaction procedure thoroughly, and controlling the chemical reaction rate and direction effectively.
- **Interfacial interaction:** Interfacial interaction significantly affects the adhesion properties of a multiphase system. The MD simulations method can help researchers understand the interfacial phenomenon and find the right ways to enhance the interfacial macroscale mechanical behaviors from the perspective of intermolecular interaction.

These functions of the MD simulation method all exist in the studies of bituminous materials. Here are some specific examples: (1) Mass transition: diffusion of oxygen, moisture, and rejuvenator in bituminous materials; (2) Mechanical response: microstructure and micromechanics of bitumen under atomic force microscopy and nanoindentation; (3) Reaction mechanism: the oxidative aging of bitumen; (4) Interfacial interaction: adhesion performance between aggregate and bitumen binder. Hence, this review will

discuss the application of MD simulation in bituminous materials in bulk, dynamic, and interfacial bitumen systems.

#### 4. Applications of MD simulations in dynamic systems of bitumen

During the preparation, construction, and service life of asphalt pavements, it is inevitable to introduce other substances into bituminous materials. For instance, the environmental oxygen and moisture mainly result in the oxidative aging and adhesion failure of bitumen, and the oxygen-moisture distinctly affects the physicochemical and mechanical bitumen properties [60]. On the other hand, the incorporation of rejuvenators or modifiers into bitumen is frequently performed to restore and improve its mechanical performance. Apart from the ultimate impacts of these external matters on the physical, morphological and mechanical properties of bituminous materials, it is also essential to fully understand their transport/diffusion behaviors for estimating the lifetime of asphalt pavements and the blending degree between rejuvenators and aged binder, which accelerates the material design of functional

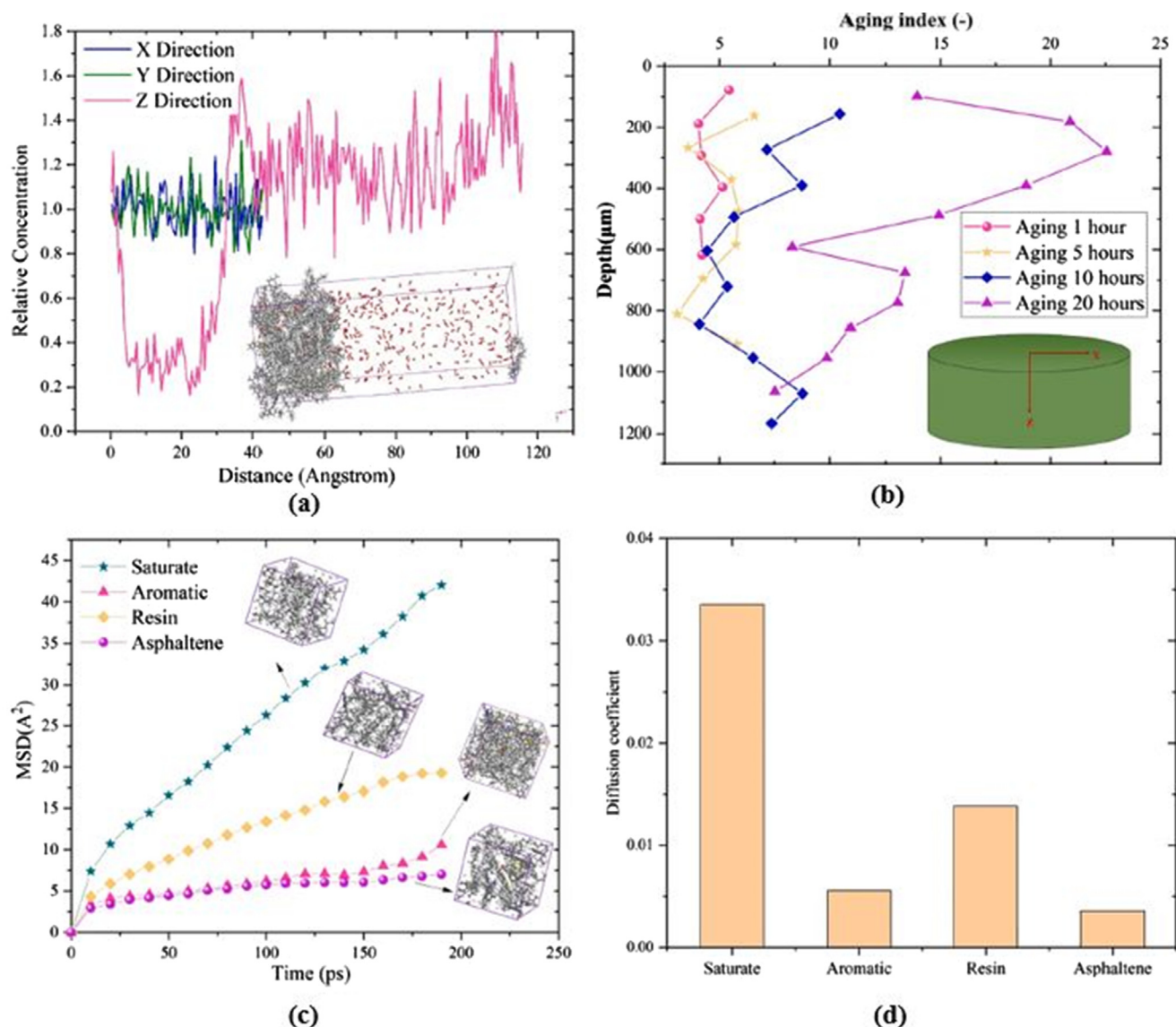


Fig. 5. MD simulation on validating the aging gradient within bitumen film [62].

aging/moisture-resistance agents and efficient rejuvenators. The diffusion coefficient is the main parameter to assess the diffusion behaviors, but it is hardly measured through the macroscale experimental tests. At the same time, the difference in transport property between different molecules in rejuvenators cannot be detected using the experiment results [61]. The molecular dynamics simulation has been proven to be an effective tool for monitoring the diffusion coefficient index and observing the molecular-level diffusive process. Thus, the diffusion coefficient values of different molecules in the multi-component substances are gauged. In this section, the application cases of MD simulations in estimating diffusion behaviors of oxygen, moisture, and rejuvenators in bituminous materials, as well as the diffusion characteristics of bitumen molecules on the aggregate surface to explain the dynamic mechanism of adhesion interfacial bitumen-aggregate systems.

#### 4.1. Diffusion behaviors of external substances and bitumen molecules

##### 4.1.1. The diffusion of oxygen and moisture in bitumen

Recently, Ma et al. [60] summarized the diffusion coefficient regions of both oxygen and moisture in bitumen and the corresponding experimental methods for measuring the diffusion coefficient parameters, such as the pressure decay, electrodynamic balance, FTIR-MIR, and gravimetric method. Although the bitumen type and test methods were different, the measured diffusion coefficient values of oxygen in bitumen were located in the region of  $10^{-11}$  to  $10^{-15}$  m<sup>2</sup>/s, while the magnitude for the diffusion coefficient of moisture differed from  $10^{-17}$  to  $10^{-9}$  m<sup>2</sup>/s. Thus, the diffusion rate of oxygen and water in bituminous materials is relatively slow, leading to the incorrect diffusion coefficient parameter measured from macroscale experiments. However, the previous successful application of MD simulation in both observation and measurement of minor gases (O<sub>2</sub>, N<sub>2</sub>, CO<sub>2</sub>) and moisture (H<sub>2</sub>O) in

polymer matrix provided the feasible idea regarding exploring the diffusion behaviors of O<sub>2</sub> and H<sub>2</sub>O in bituminous materials.

Liu et al. [62] combined the experimental and MD methods to validate the aging gradient along with the bitumen depth during the short-term laboratory aging process with the Thin Film Oven test (TFOT). The molecular oxygen-bitumen double-layers model was established (Fig. 5a), and the diffusion behavior of oxygen molecules in the bitumen layer was observed. The relative concentration in Z-direction indicated that the oxygen concentration distribution and colloidal structure in bitumen depth were inhomogeneous. From Fig. 5b, the difference in complex modulus-based aging indexes along with bitumen depth further verified that the diffusion behaviors of oxygen molecules resulted in the un-uniformity of aging degree in different depth points. Moreover, the mean square distance (MSD) and self-diffusion coefficient (D) of SARA molecules in bitumen implies that the volatilization resistance order was Asphaltene > Resin > Aromatic > Saturate (Fig. 5c and d). Although the diffusion characteristic of oxygen molecules was essential to influence the aging behavior of bituminous materials, the corresponding diffusion parameters were still measured from macroscale experimental tests, and the limited studies focused on the nanoscale evaluation of the diffusion property of oxygen using MD simulation methods.

The moisture existence form in the bituminous materials is always complicated due to the affinity between molecule molecules with the polar components (resin and asphaltene) in bitumen, fillers in asphalt mastic, and the aggregates in the asphalt mixture. Hence, the moisture susceptibility to the mechanical performance of asphalt mixture is complex, and the detailed diffusive trajectories and the interaction position of molecules are hardly detected with macroscale tests. Fig. 6 presents the representative molecular models, predicted outcomes, and molecular-scale interaction mechanisms regarding the diffusive behaviors of moisture

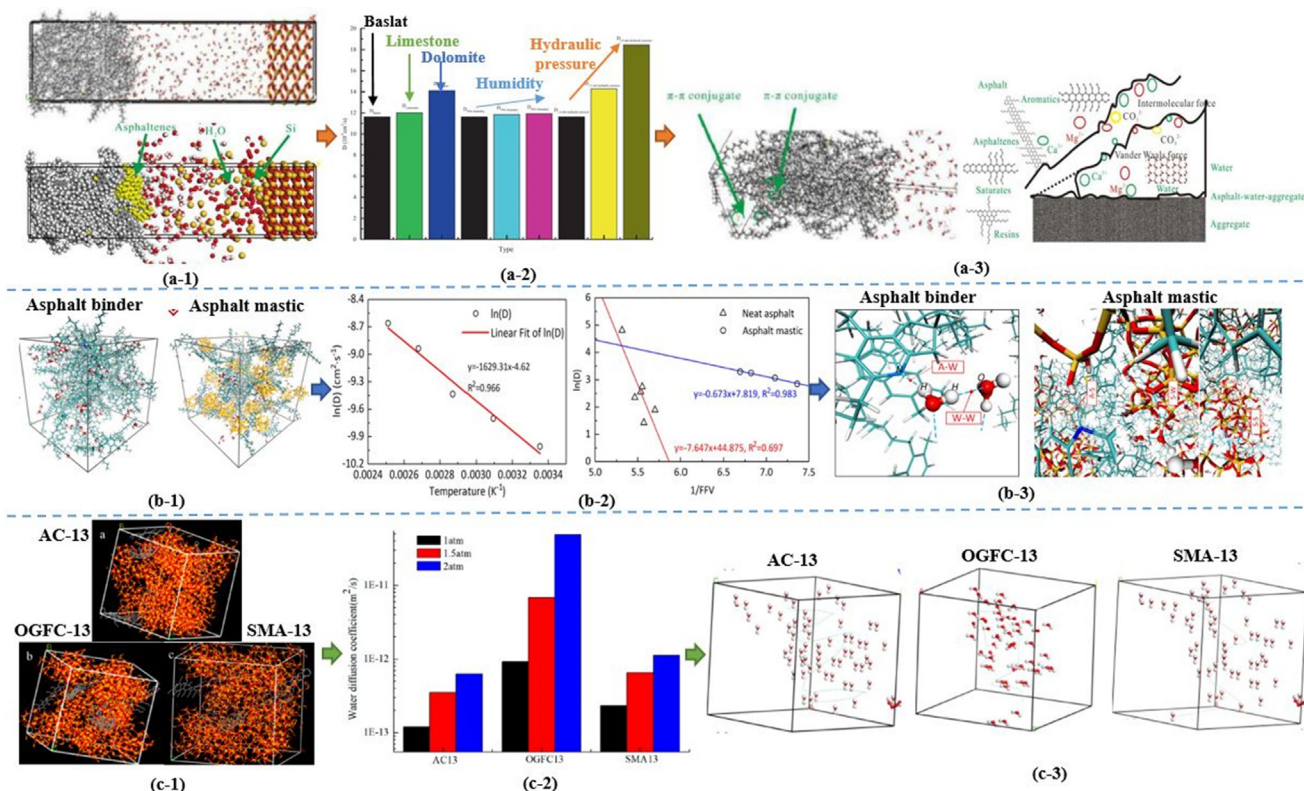


Fig. 6. MD simulation cases of the moisture diffusion in a bitumen-aggregate interface, bitumen binder, mastic, and asphalt mixtures [63–65].



molecules in various bituminous systems of a bitumen-aggregate interface (a), bulk bitumen, and mastic (b), as well as asphalt mixtures (c). As shown in Fig. 6a, Zhou et al. [63] established the nanoscale interfacial bitumen-moisture-aggregate model to investigate the influence of aggregate type, humidity, and hydraulic pressure on the diffusion characteristics of moisture molecules. The MD simulation results demonstrated that aggregate type and hydraulic pressure significantly influenced the diffusion coefficient values of moisture molecules in the bitumen-moisture-aggregate interfacial system, while the humidity factor was limited. It was interesting to note that the molecular-level moisture-induced debonding mechanism of the bituminous interfacial system was visualized and explained that the moisture molecules could form a polar layer and cover the aggregate surface. Meanwhile, the iron atoms would get away from the aggregate phase and go into the bitumen phase through the formed moisture layer, which also

influenced the thermodynamics and mechanical performance of the bulk bitumen layer.

On the other hand, Du et al. [64] conducted a nanoscale investigation on the diffusion behavior of moisture molecules in bulk bitumen and mastic systems based on the dynamic and structural parameters from MD simulations (Fig. 6b). The high moisture concentration and silica particle remarkably increased molecules' diffusion coefficient in bituminous systems. From the viewpoint of molecular structures, when the moisture dosage was low, water molecules were distributed in the bitumen model uniformly, and there was mainly hydrogen-bond interaction between moisture and bitumen molecules. However, moisture clusters were generated at high concentrations due to the predominant water-water hydrogen bonds. Moreover, the predicted cohesive energy density parameter indicated that the moisture molecules reduced the interaction among bitumen chains and increased the stripping

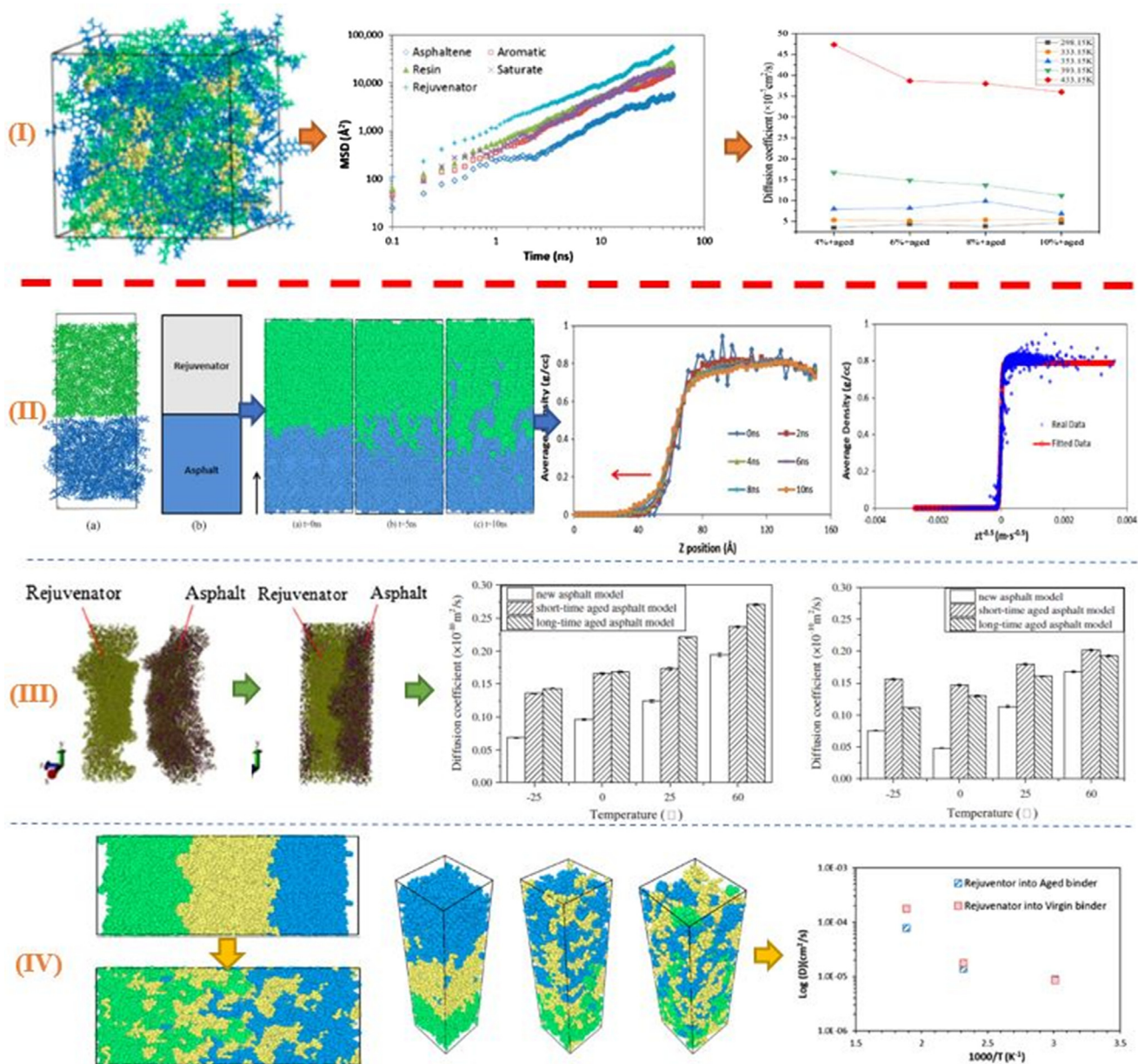


Fig. 7. The diffusion behaviors of rejuvenators at the molecular level [66,68,69,72].

potential of bituminous materials. It was revealed that the fundamental influence factors for moisture diffusion behaviors were the free volume fraction and interaction energy among bitumen chains.

Fig. 6c displays the interesting research conclusions from Zhou et al. [65]. They applied the MD simulation to explore the moisture diffusion paths, distribution, and the susceptible area of moisture damage in different types of asphalt mixtures (AC-13, OGFC-13, and SMA-13). It was reported that the air voids and pressure were both positively associated with the moisture diffusion coefficient in the asphalt mixture. As expected, the moisture diffusion path was a three-dimensional tortuous curve, and the corresponding diffusion coefficient was uneven, which had a maximum value at the z-direction because of the heavy traffic loading.

#### 4.1.2. The diffusion of rejuvenator in aged bitumen

Different rejuvenators are incorporated in the reclaimed asphalt pavement materials to restore aged bitumen's physicochemical and mechanical properties. The fast diffusive capacity of rejuvenators into an aged binder is expected as the precondition to guarantee the homogeneity of rejuvenated bitumen. However, it is difficult to measure the self-and-mutual diffusion parameters and observe the underlying interactive mechanism between the rejuvenators and bitumen molecules. The MD simulation can help researchers fundamentally understand and detect the diffusive behaviors of rejuvenators in aged bitumen from the viewpoint of the atomic level. Fig. 7 illustrates the self-diffusion (I) and inter-diffusion molecular models (II-IV) of rejuvenated bitumen together with the corresponding MD simulation results. The mixed rejuvenated bitumen model indicated that the additional rejuvenator molecules could enhance the translational mobility of SARA fractions in bitumen [66]. Cui et al. also investigated the self-diffusion behavior of rejuvenator molecules in rejuvenated bitumen systems, considering the influence of temperature and rejuvenator dosage [67]. The molecular model and corresponding results are displayed in Fig. 7(I). Compared to warm-mix temperatures, the diffusion coefficient of rejuvenators was 2–3 times larger at hot-mix temperatures, which would be weakened as the rejuvenator dosage increased.

Most existing literature focused on the inter-diffusion characteristic of rejuvenators penetrating from the rejuvenator matrix to the bitumen layer. As shown in Fig. 7(II), Xu and Wang [66] firstly explored the inter-diffusion of rejuvenator molecules in a bi-layer rejuvenator-aged bitumen model with MD simulations

and calculated the inter-diffusion coefficient of the rejuvenator based on the mass density profile in the z-direction, which agreed well with the experimental result. It was detected that the rejuvenator and bitumen molecules diffused mutually, and the diffusive rate of the rejuvenator was faster than bitumen molecules due to the smaller molecular size. Therefore, it was proposed that the inter-diffusion process was related to the molecular parameters of both rejuvenator and bitumen molecules (molecular type and concentration) and external environmental conditions (temperature and moisture dosage). Sun and Wang [68] established the bi-layered models to validate this hypothesis further and compared the inter-diffusion coefficient of different rejuvenators into aged bitumen, as illustrated in Fig. 7(III). The diffusive behavior of all rejuvenators followed Fick's second law, which varied distinctly with different molecular structures of rejuvenators. The rejuvenator with polar aromatics performed the lowest inter-diffusion rate, while the naphthene aromatics showed the best diffusive ability.

Additionally, the more oxygen-containing functional groups in long-term aged bitumen would significantly hinder the diffusivity of rejuvenators. However, a converse opinion was proposed that the diffusion speed of aged bitumen was higher than that of new bitumen [69]. The possible reason is the difference in rejuvenator type, bitumen component, and the selected forcefield. The molecular thermal motion and intermolecular force affected the diffusion driving force. Meanwhile, bituminous materials' microvoids provide space conditions and promote the diffusion capacity of rejuvenator molecules.

In practice, the fresh bitumen and rejuvenator were incorporated into the RAP mixture to improve the aged binder's high-and-low temperatures properties. Therefore, a three-layered molecular model containing rejuvenator, virgin, and aged bitumen was proposed to investigate the influence of involving rejuvenator molecules on the inter-diffusion mobility between the new and aged binders (Fig. 7 IV). The rejuvenator in the middle layer improved the diffusion speed of both fresh and aged bitumen molecules and increased their blending degree, which was more evident at high temperatures. A similar conclusion was also drawn by Ding et al. [70], who employed the rotational viscometer (RV), gel permeation chromatography (GPC), and MD simulation methods to investigate the diffusion process between virgin and aged bitumen molecules considering the rejuvenator effect. They also found that virgin and aged binders did not superimpose the viscosity and molecular weight of the mixed binder. Meanwhile, the

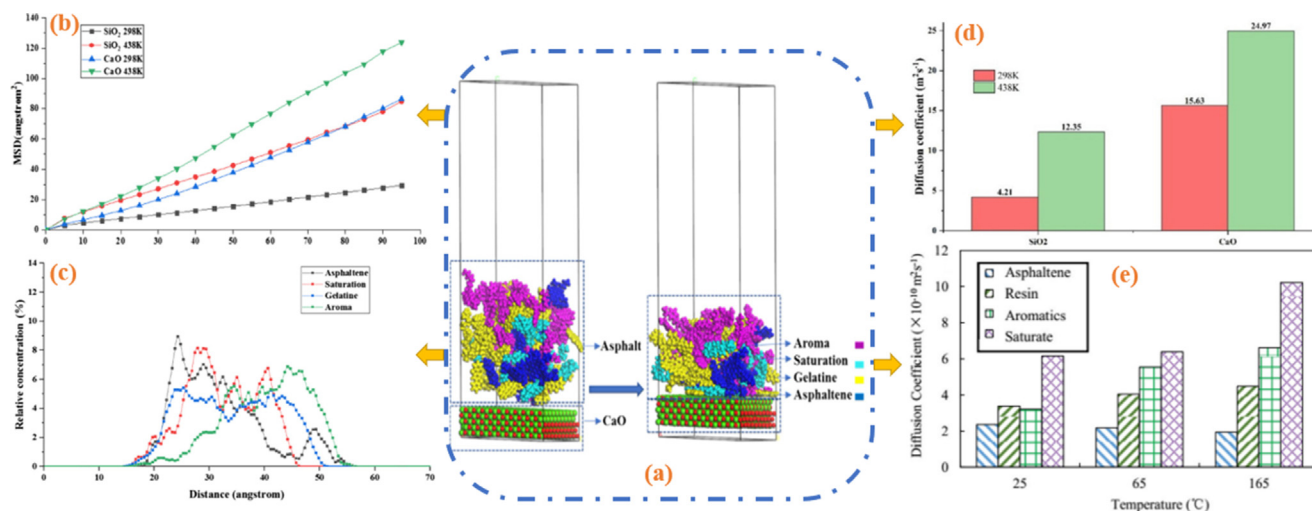


Fig. 8. The diffusion behaviors of bitumen molecules on the aggregate surface [64,73,74].



asphaltene and resin molecules tended to form molecular aggregates, which were influenced by both the aging level and the chemical compositions of bitumen. Furthermore, during the inter-diffusion process between virgin and aged bitumen, it was verified that the diffusion of large molecules in bitumen was critical. Meanwhile, the diffusion coefficient parameters of virgin bitumen molecules were not only related to the diffusive ability but also influenced by the molecular characteristics of aged bitumen molecules (such as the free volume fraction and intermolecular interaction). Ding et al. [71] proposed and calculated the volume diffusion coefficients of virgin-virgin, aged-aged, and bio-aged-aged bitumen layers and summarized that the aging of the bitumen model led to a reduction in diffusion efficiency. At the same time, the bio-rejuvenator could effectively recover aged bitumen molecules' diffusive capacity and dispersion uniformity.

#### 4.1.3. The diffusion of bitumen components on the aggregate surface

The diffusive behaviors of bitumen molecules on the aggregate surface were studied using MD simulation to explore and compare their dynamic adhesion capacity with aggregate flat. Fig. 8 demonstrates the bitumen-aggregate interfacial system and corresponding MD simulation dynamic parameters, such as the MSD, relative concentration, and diffusion coefficient. The sequence of diffusion speed for bitumen molecules on the aggregate surface was reported as saturate > aromatic > resin > asphaltene. As expected, the increasing temperature would promote the diffusion rate of bitumen molecules. In addition, it was reported that the aggregate compositions influenced the diffusion behaviors. Guo et al. [73] found that the diffusion coefficients of bitumen molecules exhibited the most prominent values on the surface of  $\text{Al}_2\text{O}_3$ , while the temperature sensitivity was the maximum on the CaO surface. The diffusion coefficient ranking of bitumen molecules and temperature dependence was verified by Du and Zhu [64], who also analyzed the adhesion energy between the bitumen molecules and aggregate. The findings revealed that the van der Waals energy played a leading role in forming the strong physisorption of bitumen molecules on the mineral aggregate surface. The ranking of adhesion energy between the SARA fractions and quartz was asphaltene > resin > saturate > aromatic. In contrast, the work of adhesion between bitumen and aggregate oxides ranked as follows:  $\text{MgO} > \text{CaO} > \text{Al}_2\text{O}_3 > \text{Fe}_2\text{O}_3 > \text{SiO}_2$ . Huang et al. [74] analyzed the interfacial diffusion characteristics by calculating the dipole moment of bitumen and aggregate molecules according to the molecular orientation theory and thought that the fundamental reason for the adhesion bonding was the polarity of both bitumen and aggregate molecules. The high polarity of asphaltene and resin molecules promoted their interfacial interaction with polar aggregates.

## 5. Self-healing characters of bituminous materials

### 5.1. Self-healing phenomenon and potential mechanism

The fatigue behavior and life span of bituminous materials attract more attention to researchers, and the mechanical performance deteriorations of bitumen were due to the crack initiation and propagation [75]. Moreover, the bitumen binder shows self-healing behavior because of its viscoelastic characteristics [76]. Therefore, amounts of experimental works have been conducted to assess the macroscale self-healing ability of bitumen binder, mortar, or asphalt mixture by comparing their mechanical parameters with and without the self-healing process. However, a thorough understanding of the healing mechanism of bitumen is limited only based on the macroscale measurements, which is essential to find the key factors and design effective additives to

accelerate the self-healing behavior and prolong the life span of asphalt pavement.

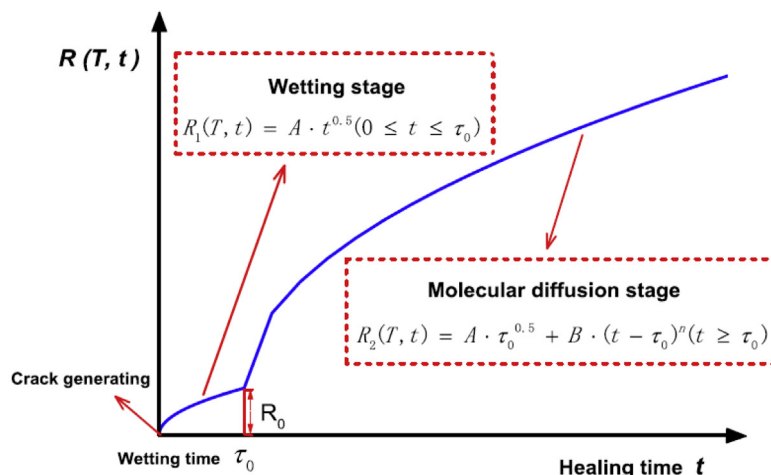
As defined, the self-healing process is accompanied by the disappearance of existing cracks and restoration of the mechanical performance of materials. Regarding the internal mechanism, there were five molecular-level steps during the self-healing of bitumen: surface arrangement, surface approach, wetting, diffusion, and randomization [77,78]. These five steps can be divided into two categories, including molecular motion (free energy change) and rearrangement (bond restoration). When the systematic energy is sufficient, the molecules at the crack surface will get over the energy barrier from the surface's attractive force and movement flow in the opposite direction. And the cracks disappeared gradually, followed by further intrinsic healing, which contributed to the strength-recovery of broken bituminous materials. Sun et al. [79] also explained the self-healing mechanism of bitumen from the perspectives of wetting and molecular diffusion stages (Fig. 9a). Furthermore, they utilized the fluorescence microscope (FM) method to observe the variation of the crack area and calculate the healing index during the self-healing process of bitumen (Fig. 9b).

Fig. 9c briefly describes the self-healing mechanism of bitumen at the molecular level. First, in the wetting stage, the molecules in separated bitumen surfaces diffuse freely and start contact because of the capillary force. Then, during the molecular diffusion stage, these molecules would further diffuse and entangle to cure the microcracks and restore the damaged bitumen system's uniformity and mechanical properties. Additionally, the whole self-healing process was strongly associated with the diffusion capacity of bitumen molecules, and it was also significantly influenced by the molecular structure and external temperature.

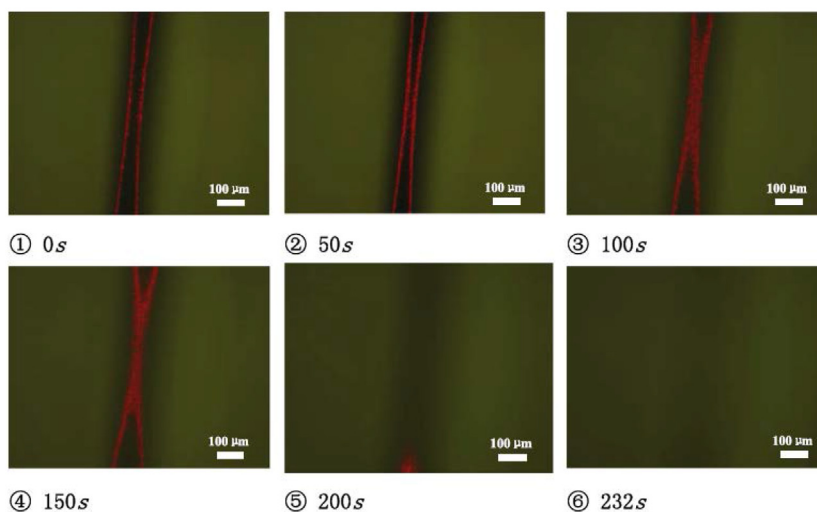
### 5.2. Molecular-scale self-healing models

As aforementioned, the MD simulation technique efficiently illustrates the molecular-scale diffusion trajectory of bitumen molecules. To further verify the potential correlations between the self-healing ratio and chemical structure of bitumen molecules (chain length and chain branching), Bhasin et al. [80] conducted an MD simulation on both average and three-components molecular models of bitumen with a COMPASS force field. To simulate the healing procedure occurring across the interface of a crack, a vacuum layer was inserted between two bitumen layers (shown in Fig. 9d). Afterward, the MD simulation with an NPT ensemble was performed for 50 ps at 298 K. The self-diffusion coefficient values of bitumen models with a different  $\text{CH}_2/\text{CH}_3$  ratio and methylene plus methyl hydrogen to carbon ratio (MMHC) were calculated based on the variety of the mean square distance (MSD) parameter outputted from MD simulations. The conclusions from an MD simulation were consistent with the experimental findings that the diffusivity at the cracked molecular interface of bitumen systems enlarged with an increment in the chain length ( $\text{CH}_2/\text{CH}_3$  ratio) and a decrease in the chain branching (MMHC ratio).

Besides, Qu et al. [81] built the aggregate-bitumen self-healing molecular model (Fig. 9e) with a six-fraction bitumen model and studied the self-healing behavior of bitumen models. And they mentioned that the crack with low width exhibited a tremendous self-healing potential, which the increment could accelerate in temperature and with the addition of graphene. However, it was revealed that the molecular agglomeration and incorporation of aggregate hindered bitumen molecules' diffusion and self-healing rate. Overall, the "compression" of model volume and the "stretching" of bitumen molecules are the main reasons for the disappearance of the vacuum micro-crack inside the whole bitumen system during MD simulations.



(a) Strength formation process during bitumen healing



(b) The FM images of the crack healing process of bitumen

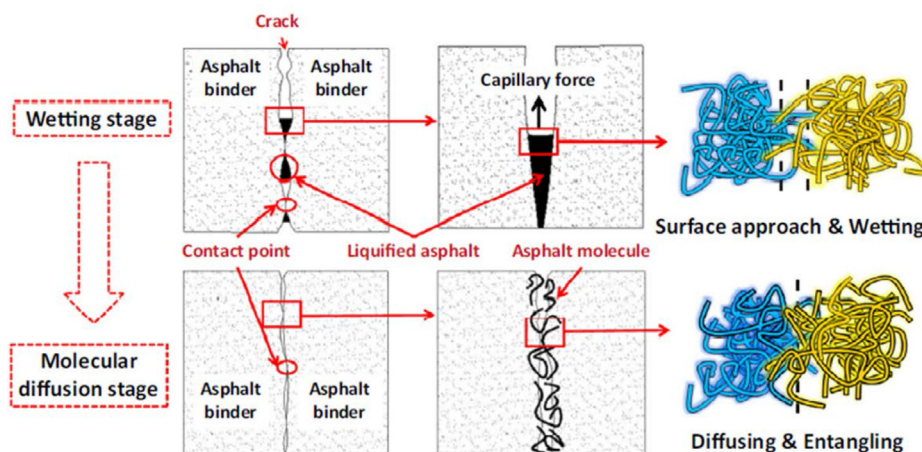
Fig. 9. The self-healing molecular layer models of bitumen.

### 5.3. Multiscale evaluation on self-healing performance

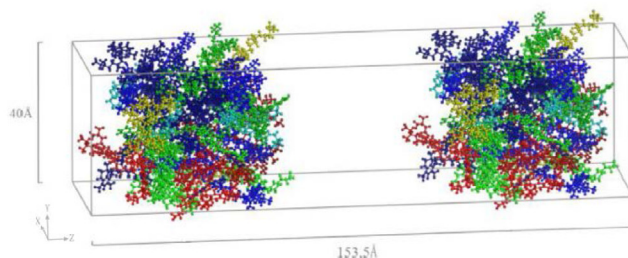
Sun et al. [82] combined the macroscale fatigue-rest-fatigue and MD simulation methods to implement a multiscale study on the self-healing properties of neat and SBS-modified bitumen. Three effective indicators (diffusion coefficient, activation energy, and pre-exponential factor) predicted from MD simulations were proposed to assess the self-healing capacity of various bitumen systems under different temperature conditions. The results demonstrated that the MD simulation findings were qualitatively identical to the experimental conclusions that the SBS modified bitumen showed a better self-healing ability than pure bitumen. In the meantime, they established the average molecular models of four bitumen with different penetration grades of PEN20, PEN50, PEN70, and PEN100. After the phase transition temperature ranges of these four binders were determined by the differential scanning calorimeter (DSC) test, the self-healing MD simulations of bitumen molecular models were conducted at different temper-

atures. It was reported that although high-temperature conditions would be beneficial to improving the diffusion rate and self-healing capacity of bitumen molecules, they should be controlled at 40.3–48.7 °C to prevent permanent deformation.

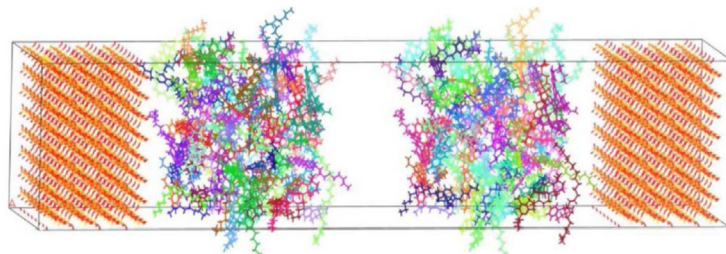
From the viewpoint of mechanical characterizations, the self-healing performance of bitumen binder is generally evaluated through a “damage-rest-damage” test, and the ratio of mechanical parameters (modulus and strength) or lifespan with and without the self-healing rest process was monitored. The self-healing process of bitumen consists of cohesion failure, crack development, and strength recovery phenomena. However, most MD simulations focused on the molecular mobility of bitumen molecules and the disappearance rate of an existing crack in a bitumen model during the self-healing procedure. Sun and Wang [76] investigated the self-healing properties of a bitumen model with MD simulations. The bitumen’s molecular model was first subjected to an external tension procedure, and the cohesive failure trend at an atomic scale was observed. Afterward, the external force was withdrawn,



(c) Illustration of self-healing mechanism of bitumen



(d) Bitumen-bitumen self-healing layer model



(e) Aggregate-bitumen-bitumen-aggregate self-healing layer model

Fig. 9 (continued)

and the self-healing capacity was investigated by observing the cracked surfaces and tensile strength as a function of healing time. The cohesion failure of the bitumen molecular model could be observed under the pull-off simulation (shown in Fig. 10), and the stress-strain curve was drawn. The crack width increased distinctly as the pull-off simulation time prolonged. The cohesive strength of the bitumen model was reported as 241.2 MPa, which was consistent with the experimental result. The molecular-level self-healing of the cracked bitumen model could be detected when the external force was withdrawn. Fig. 10c presents the interface movement and crack width disappearance phenomenon during the self-healing MD simulations. Similar to the macroscopic test, the pull-off simulation of the self-healed bitumen model has been carried out again. The healing ratio could be calculated by dividing the tensile strength of healed bitumen through the initial tensile strength. The rapid surface wetting-induced recovery and slow diffusion stages could be captured. However, a tensile strength of

damaged bitumen may not be completely recovered when the crack disappears, and the healing ratio significantly relies on the initial damage degree (crack width) and temperature.

#### 5.4. Influence factors on self-healing behavior

The impacts of crack width, temperature, healing agent, polymer modifiers, and aging on the self-healing behaviors of bituminous materials have been explored initially with the MD simulation method. Shen et al. [83] reported that the damage degree (or crack width) and temperature directly showed a negative and positive influence on the self-healing capacity of bitumen binders, respectively. Additionally, Yu et al. [84] found that the effect of nano-crack width was more evident than the temperature variation. Besides, aging would deteriorate the self-healing capacity, and thus more activation energy or longer time was required to complete the diffusion flow procedure. Moreover, the AFM and



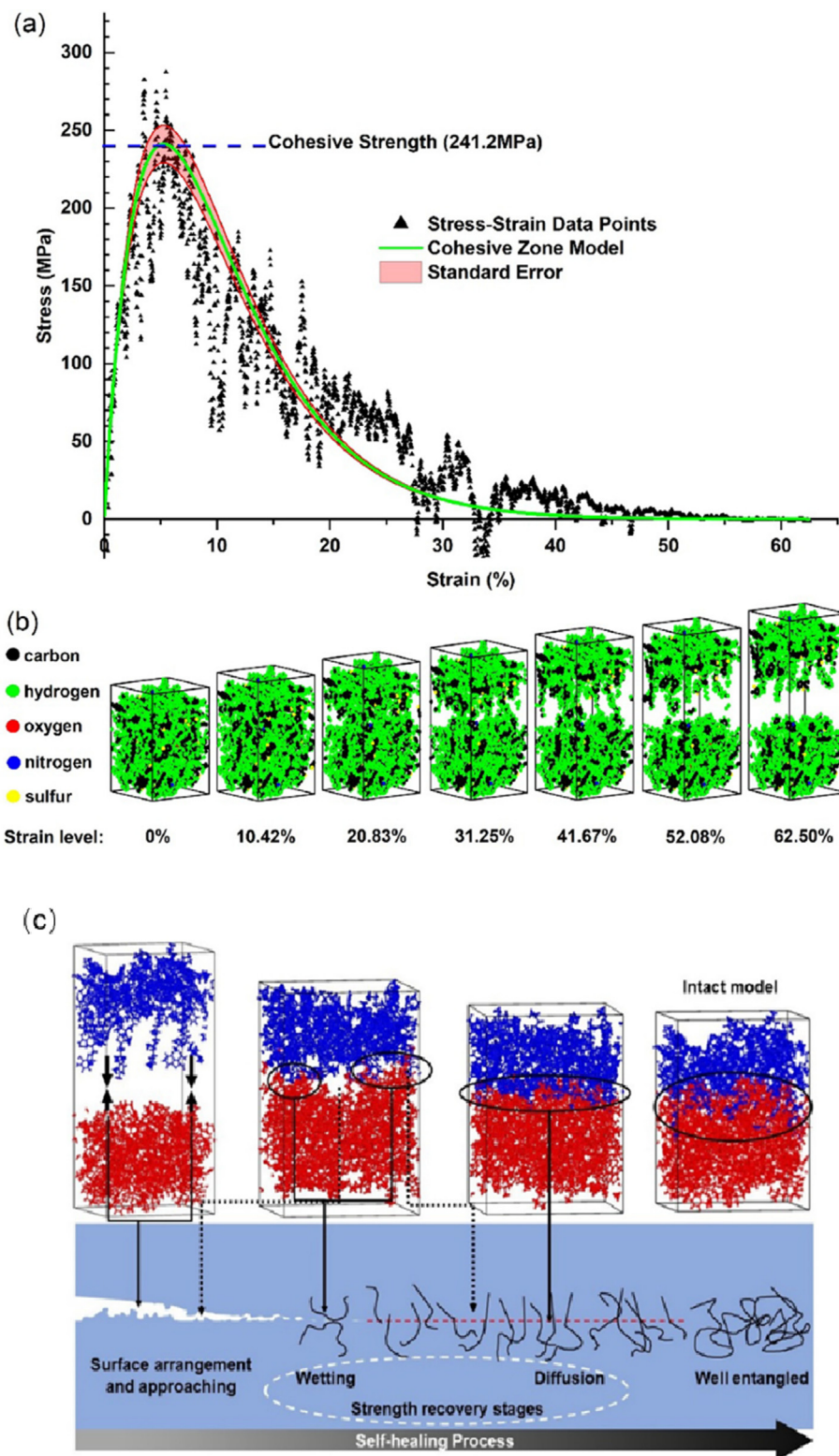


Fig. 10. The crack development and disappearance of the bitumen molecular model during the pull-off and self-healing processes.

SEM microscopic observations implied that an aged bitumen showed more micro-voids and larger nano-crack width than a pure bitumen. According to the density variety as a function of simulation time, the self-healing behavior of a bitumen molecular model could be divided into three steps: initial turbulent stage, distance self-healing stage, and strength self-healing stage, which

corresponds to the rearrangement, wetting, and molecular diffusion mechanism, respectively.

Experimental and MD simulation results illustrate that temperature and aging affect the self-healing properties of bitumen. To accelerate the diffusion rate of molecules on the cracked bitumen surface and prolong the service life of asphalt roads, heating and

softening are the leading solutions. The novel techniques of induction heating and microwave heating have been developed to increase the temperature of cracked asphalt roads and promote the self-healing process of bitumen. At the same time, the embedded rejuvenator encapsulation method is recommended to facilitate the healing capacity of aged bitumen. When the crack occurred, the soft oily additive (rejuvenators) in the capsule would be released and diffused into the aged bitumen, thus increasing the low molecular-weight molecule proportion and free volume in the bitumen system. The intrinsic mechanism regarding the encapsulation influence on the self-healing capacity of bitumen is associated with the improvement in diffusion behavior of bitumen molecules after rejuvenators are incorporated. Hence, the encapsulation method significantly depends on developing the rejuvenation technology of bitumen. The MD simulation findings by Shu et al. [85] suggested that the release of sunflower oil in the capsule reduced the viscosity and improved the wetting rate of bitumen. In conclusion, based on the actual results from MD simulation, more efficient healing methods and additives could be developed to promote the self-healing capacity of bitumen binder and increase the service life of asphalt pavement.

He et al. [86] concentrated on the diffusion rate of each component molecule in the self-healing molecular models of virgin bitumen, aged, and SBS-modified binders. During the self-healing MD simulation of bitumen models, the compression of system volume and the stretching of bitumen molecules contributed to the disappearance of the micro-cracks, mainly driven by the Van der Waals forces between non-bonded molecules. As expected, the diffusion rate of asphaltene molecules was the lowest, while the diffusion coefficient of saturates was the highest. The considerable average molecular weight and strong interaction of asphaltene obstacle its molecular motion and diffusion capacity. Compared to virgin bitumen, the aging process reduced the diffusion ability of bitumen molecules, whereas the addition of SBS exhibited the contrary effect. They also utilized MD simulation to estimate the enhancement influence of two healing agents (plant oil and aromatic oil)

on the micro-crack self-healing in virgin and short-aged bitumen models [87]. The incorporation of healing agents significantly promotes the healing rate and prolongs the life span of asphalt roads. Furthermore, compared to plant oil, the improvement effect of aromatic oil on the healing capability and structural uniformity of the short-aged bitumen system was superior. Lastly, the healing temperature for virgin and short-aged binders was recommended to be above 15 °C and 45 °C, respectively. Similarly, Tian et al. [88] concluded that the four types of repairing agents could accelerate the intermolecular diffusion of bitumen molecules and enhance the recovery of the bitumen model's mechanical property (shear modulus). Moreover, the MD simulation results denoted that the light and the long chain-like small molecule were more suitable as the repairing agent of microcapsules because of their high efficiency in accelerating the self-repairing process of bitumen.

## 6. Applications of MD simulations in interfacial bituminous systems

It is well-known that the asphalt mixture is composed of a bitumen binder and aggregate. The interfacial properties of bitumen-aggregate are of great significance to the whole asphalt mixture's cohesion and adhesion failure resistance. The primary technology to evaluate the interfacial properties of asphalt mixture is through the macroscale mechanical methods, such as the boiling test, pull-off test, and Cantabro abrasion test [89,90]. Although the advanced surface free energy and Atom Force Microscopy (AFM) methods are proposed, these experimental methods are cost-and-time consuming. On the other hand, theories from the mechanic, chemical reaction, surface free energy, surface structure, weak boundary, molecular orientation, and electrostatic aspects are proposed. Nevertheless, the underlying interaction mechanism between bitumen and aggregate is still unclear, especially at an atomic level [91]. To this end, the molecular dynamics simulation method has been developed and utilized in the bitumen-aggregate interfacial systems to understand adhesion failure and moisture damage mecha-

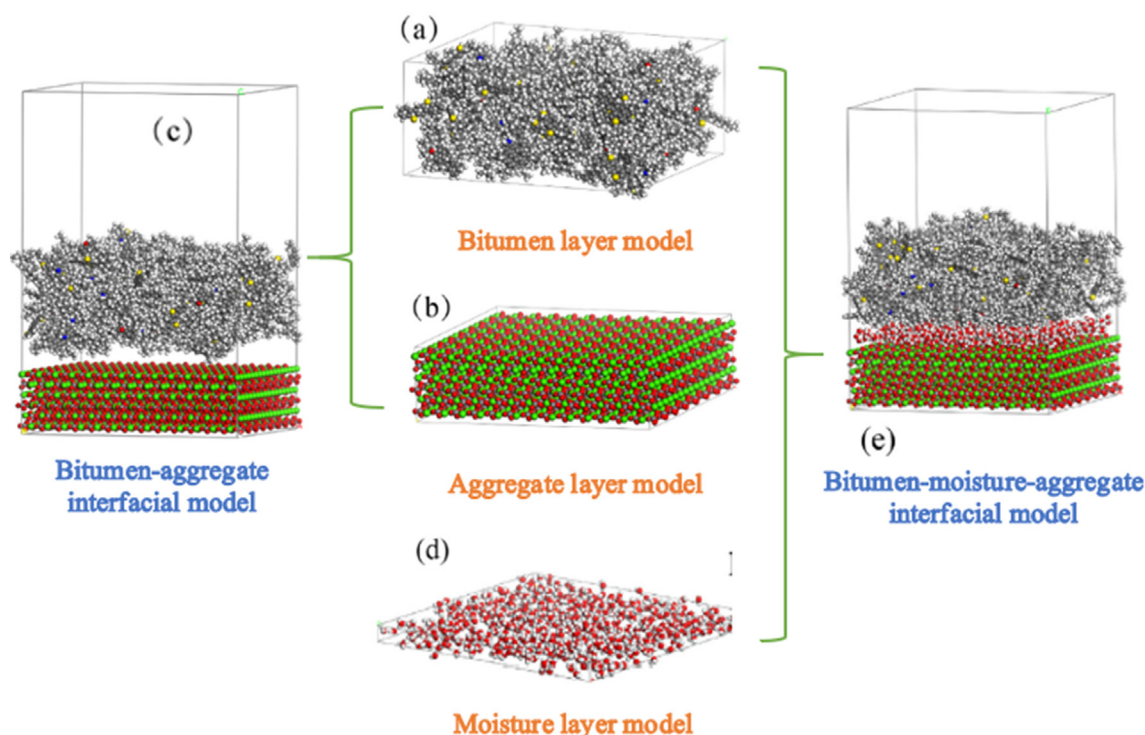


Fig. 11. The establishment of bitumen-(moisture)-aggregate interfacial molecular models [93].

**Table 1**

The overview of aggregate and bitumen models, influence factors, and evaluation parameters in interfacial systems.

Aggregate models	Bitumen models and selected forcefield	Influence factors	Evaluation parameters	Ref
Calcite (CaCO <sub>3</sub> );	<b>Bitumen models:</b> (1) AAA-1 12-component bitumen;(2) SiO <sub>2</sub> asphalt mastic; <b>Forcefield:</b> COMPASS;	(a) Moisture: 200 water molecules; (b) Temperature: 298.15 and 343.15 K;	<b>Validation:</b> Cohesive energy density; Density; Glass-transition temperature; <b>Structural:</b> Radial distribution function; Relative concentration; <b>Dynamics:</b> Mean square distance; <b>Interfacial:</b> Work of adhesion;	[94]
MgO; CaO; Al <sub>2</sub> O <sub>3</sub> ; Fe <sub>2</sub> O <sub>3</sub> , SiO <sub>2</sub> ; Na <sub>2</sub> O;	<b>Bitumen models:</b> AAA-1 12-component bitumen; <b>Forcefield:</b> COMPASSII;	(a) Temperature: 273.15, 298.15, 323.15, 348.15 and 373.15 K;	<b>Interfacial:</b> Binding energy; Work of adhesion; <b>Dynamics:</b> Diffusion coefficient; Mean square distance; Activation energy;	[110]
Silica (SiO <sub>2</sub> )	<b>Bitumen model:</b> AAA-1 12-component bitumen (CNOOC 90 <sup>#</sup> and Panjin 90 <sup>#</sup> ); <b>Forcefield:</b> COMPASS;	(a) Short and long-term aging; (b) Temperature: 0, -5, -15, -25 and -35 °C;	<b>Validation:</b> Density; <b>Interfacial:</b> Interfacial energy; <b>Dynamics:</b> Mean square distance; Diffusion coefficient;	[108]
Silicon (SiO <sub>2</sub> )	<b>Bitumen model:</b> Three-component bitumen; <b>Forcefield:</b> Amber Cornell Extension Force Field (ACEFF);	(a) Temperature: 273.15, 298.15, 318.15, 338.15 and 353.15 K;	<b>Dynamics:</b> Mean square distance; <b>Interfacial:</b> Contact angle;	[95] [109]
Steel slag (C <sub>3</sub> S);Silicon (SiO <sub>2</sub> ); Calcite (CaCO <sub>3</sub> );	<b>Bitumen model:</b> AAA-1 12-component bitumen; <b>Forcefield:</b> COMPASS;	(a) Moisture: 200 water molecules;	<b>Validation:</b> Density; Cohesive energy density; Solubility parameter; Glass transition temperature; <b>Structural:</b> Radial distribution function; Relative concentration; <b>Interfacial:</b> Work of adhesion; Debonding work;	[96]
Steel slag (C <sub>3</sub> S);	<b>Bitumen model:</b> AAA-1 12-component bitumen; <b>Forcefield:</b> COMPASS II;	(a) Temperature: 253.15, 273.15, 298.15, 333.15 and 353.15 K; (b) Moisture: 200, 400, and 600 water molecules;	<b>Dynamics:</b> Mean square distance; Diffusion coefficient; <b>Structural:</b> Radial distribution function; Relative concentration; <b>Interfacial:</b> Work of adhesion;	[97]
Basalt (SiO <sub>2</sub> ); Steel slag (CaO.(Al <sub>2</sub> O <sub>3</sub> ) <sub>2</sub> .(SiO <sub>2</sub> ) <sub>2</sub> ); Andesite (SiO <sub>2</sub> );	<b>Bitumen model:</b> Three-component bitumen;	–	<b>Interfacial:</b> Adhesive energy; Thermal energy; Failure energy ( $\Delta E = E_{\text{interface}} - E_{\text{cohesive}}$ ); <b>Dynamics:</b> Mean square distance; Diffusion coefficient;	[98]
Silicon (SiO <sub>2</sub> );	<b>Bitumen model:</b> AAA-1 12-component bitumen; <b>Forcefield:</b> Optimized Potentials for Liquid Simulations (OPLS);	(a) Pull-off loading rate: 10, 20 and 30 m/s; (b) Temperature: 0, 25 and 80 °C;	<b>Validation:</b> Density; Glass transition temperature; <b>Interfacial:</b> Stress-separation responses (Cohesive zone law; peak stress and work of separation);	[72]
Silicon (SiO <sub>2</sub> );	<b>Bitumen model:</b> AAA-1 12-component bitumen; <b>Forcefield:</b> Polymer consistent force field (PCFF);	(a) Model size; (b) Loading rate; (c) Asphalt film thickness: 33, 67, 100, and 133 Å; (d) Moisture content:100, 200, 300 water molecules;	<b>Validation:</b> Density; Cohesive energy density; Solubility parameter; <b>Interfacial:</b> Stress-Separation curve (work of separation);	[99]
Silicon (SiO <sub>2</sub> );Calcite (CaCO <sub>3</sub> );	<b>Bitumen model:</b> Three-component bitumen; <b>Forcefield:</b> COMPASSII;	(a) Temperature: 263, 298 and 333 K; (b) Moisture: 100, 150, and 200 water molecules;	<b>Validation:</b> Density; Surface free energy; Work of cohesion; Cohesive energy density; Solubility parameter; <b>Interfacial:</b> Work of adhesion; Work of debonding; Energy ratio;	[92]
Quartz (SiO <sub>2</sub> );	<b>Bitumen model:</b> Three-component bitumen; <b>Forcefield:</b> Consistent-valance force field (CVFF);	–	<b>Mechanical:</b> Quartz elastic constants; <b>Interfacial:</b> Stress-strain relationship of the asphalt-quartz interface;	[100] [101]
Silicon (SiO <sub>2</sub> );	<b>Bitumen model:</b> AAA-112-component bitumen; <b>Forcefield:</b> ReaxFF;	(a) Temperature: -40, -20, 0, 25 and 60 °C; (b) Aging of bitumen molecules;	<b>Interfacial:</b> Adhesion energy; Work of separation; <b>Mechanical:</b> Maximum stress and force;	[102]
SiO <sub>2</sub> ; CaO; Al <sub>2</sub> O <sub>3</sub>	<b>Bitumen models:</b> AAA-1, AAK-1 and AAM-1 12-component bitumen; <b>Forcefield:</b> COMPASSII;	(a) Mineral surface directions: 001, 100 and 011; (b) Electrostatic; structure and hydroxyl; (c) Technique details: Summation method; Vacuum slab; Chemical bonds;	<b>Interfacial:</b> Binding energy; Work of adhesion; <b>Structural:</b> Radial distribution function; <b>Energetic:</b> Potential energy;	[103]
Al <sub>2</sub> O <sub>3</sub> ;	<b>Bitumen model:</b> Four-component bitumen; <b>Forcefield:</b> COMPASS;	(a) Temperature:25, 65 and 165 °C;	<b>Mechanical:</b> Bulk, shear, and Young's modulus; Poisson's ratio; Compression coefficient; <b>Dynamics:</b> Mean square distance; Diffusion coefficient;	[104]
MgO; CaO; Al <sub>2</sub> O <sub>3</sub> ; Fe <sub>2</sub> O <sub>3</sub> , SiO <sub>2</sub> ;	<b>Bitumen model:</b> Four-component bitumen; <b>Forcefield:</b> COMPASS;	(a) Temperature: 25, 65 and 165 °C;	<b>Structural:</b> Concentration distribution (concentration peak and position);	[105]
SiO <sub>2</sub> ; CaO;	<b>Bitumen model:</b> AAA-1 12-component bitumen; <b>Forcefield:</b> COMPASS;	(a) Temperature: 298 and 438 K	<b>Validation:</b> Density; Solubility parameters; <b>Dynamics:</b> Mean square distance; Diffusion coefficient; <b>Energetic:</b> Change of energy; <b>Structural:</b> Radial distribution function; Relative concentration; Dipole moment	[74]



Table 1 (continued)

Aggregate models	Bitumen models and selected forcefield	Influence factors	Evaluation parameters	Ref
Silicon (SiO <sub>2</sub> ); Calcite (CaCO <sub>3</sub> );	<b>Bitumen model:</b> AAA-1 12-component bitumen; <b>Non-equilibrium molecular dynamics (NEMD) simulations;</b>	(a) Temperature: 300–500 K; (b) SBS content: 7.9 %, 20 %; (c) SBS structure: Linear; Radial;	<b>Validation:</b> Density; Glass transition temperature; Thermal conductivity; <b>Interfacial heat transport:</b> Energy; temperature; Kapitza thermal resistance;	[106]

nisms fundamentally. At the same time, the influence of aggregate characteristics, bitumen properties, and external environmental factors (temperature and moisture) on the adhesion behaviors of the bitumen-aggregate biphasic system could be estimated with MD simulation at the nanoscale. This section first introduces the basic knowledge regarding the application of MD simulation in bitumen-aggregate interfacial systems, including establishing interfacial molecular models, influence factors, and evaluation parameters. Afterward, the influence factors of the bitumen-aggregate interfacial system are summarized here.

## 6.1. Basic knowledge

### 6.1.1. Interfacial molecular models

Before running the MD simulation, the establishment of representative molecular models for bitumen or bitumen-aggregate systems is significantly essential. Fig. 11 depicts the formation process of interfacial molecular models. Firstly, the bitumen and aggregate layer models were built separately by removing the periodic boundary condition in the z-direction. Meanwhile, the surface free energy of the bitumen phase could be obtained by calculating the difference in potential energy between the bulk and confined models, which is a vital parameter in assessing the cohesive cracking property of the bitumen binder [92]. Regarding the aggregate layer model, the crystal unit cell of the mineral substrate was first selected and cleaved along one miller plane to expose the contact surface. Afterward, the existing crystal surface cell was extended to build an orthogonal mineral supercell. Lastly, a vacuum layer was added to ensure the periodic boundary condition. Finally, geometry optimization and MD simulations were conducted on the bitumen and aggregate layer model to minimize the energy and obtain the corresponding equilibrium models.

The bitumen-aggregate interfacial model could be built by putting the bitumen layer model on the aggregate layer model (Fig. 11c). A vacuum layer was incorporated at the top of the interfacial model to create the periodic boundary condition. After a geometry optimization step, the interfacial system was subjected to the molecular dynamics procedure with selected simulation conditions of Forcefield, time step, ensemble (NVT normally), temperature, and the number of steps. During an NVT dynamics simulation, the bitumen components thoroughly diffused and interacted with the crystal molecular on the aggregate surface. The fully-equilibrium interfacial model was further used to evaluate the adhesion performance through the parameters of the interaction energy and work of adhesion.

The moisture sensitivity is the central issue to the adhesion failure of the asphalt mixture. The atomic-scale moisture damage mechanism on the bitumen-aggregate interfacial system was investigated with MD simulation technology. The aggregate is more hydrophilic than bitumen, and the moisture molecule interacts strongly with crystal molecules on the aggregate surface, which would weaken the interaction force between bitumen and aggregate molecule. To figure out the moisture influence, the

aggregate-moisture-bitumen tri-layers model (Fig. 11e) was established by inserting the thin-layer moisture model (Fig. 11d) into the bitumen-aggregate interface. The simulation and analytical methods are the same as the bitumen-aggregate model. In contrast, the moisture damage resistance of the bitumen-aggregate system is assessed by the debonding and energy ratio parameters.

### 6.1.2. Influence factors

Based on both experiments and MD simulations literature, several factors were considered to influence the interfacial bonding between bitumen and aggregate, including the properties of materials (both bitumen and aggregate phases), external conditions (temperature, moisture, loading rate) as well as the simulation environment (force field, model size). Table 1 lists some typical cases regarding the utilization of MD simulation on the bitumen-aggregate interfacial systems. The commonly-used aggregates in asphalt roads are acidic granite and weakly alkaline limestone, of which the chemical composition is Silicon (SiO<sub>2</sub>) and Calcite (CaCO<sub>3</sub>), respectively. In addition, other types of aggregate models were also established and studied, such as the metal oxides (MgO, CaO, Al<sub>2</sub>O<sub>3</sub>, Fe<sub>2</sub>O<sub>3</sub>, and Na<sub>2</sub>O), Albite (NaAlSi<sub>3</sub>O<sub>8</sub>), Microcline (KAlSi<sub>3</sub>O<sub>8</sub>), and steel slag (C<sub>3</sub>S and CaO(Al<sub>2</sub>O<sub>3</sub>)<sub>2</sub>(SiO<sub>2</sub>)<sub>2</sub>) [94–106]. Apart from the crystal components, the aggregate mineral surface anisotropy and roughness (texture structure) also play an essential role in the adhesion interaction between aggregate and bitumen.

Given the development and accuracy improvement of molecular models of bitumen, the 12-component molecular model proposed by Li and Greenfield [107] is mainly adopted to construct the bitumen layer model in the aggregate-bitumen interfacial systems [57,72,94,96,97,99,103,108]. In some studies, the three-component [92,95,98,100,101,109] and four-component [104,105] molecular models were also utilized to represent the bitumen structure. However, the difference in simulation outputs from the aggregate-bitumen interfacial systems with various bitumen models has not been studied and compared.

Regarding the influence of stimulation parameters, there are a few relevant researches. Here is only a list of the types of forcefield in different bitumen-aggregate interface studies. It can be found that the COMPASS (or COMPASS II) forcefield is always chosen to conduct the MD simulation on the bitumen-aggregate interfacial systems [108,74,110,92,94,96,97,103–105]. Other types of forcefield were applied in a few studies, including the Amer Cornell Extension Forcefield (ACEFF) [95,109], Optimized Potential for Liquid Simulations (OPLS) [72], and Polymer consistent Forcefield (PCFF) [99], and Consistent Valance Forcefield (CVFF) [100,101]. Ma et al. [103] investigated the influence of simulation details on the simulation results of bitumen-aggregate interfacial systems. They recommended that the geometry optimization of the whole model was not necessary. At the same time, the effects of adding a vacuum slab to the cleaved aggregate surface and deleting the chemical bonding could not be ignored. Furthermore, the Ewald and atom-based methods were proposed for the energy summation of electrostatic energy and van der Waals energy, respectively.

Table 1 also displays the influence factors on the interfacial bonding of aggregate-bitumen systems regarding the materials components and external environmental conditions. The interfacial model is composed of the aggregate and bitumen phases, and the influence of their material constituents is of great significance. In terms of the bitumen phase, the aging (short and long-term aging) [102,108,111], modification (polymer, filler, and bio-oil) [106,112], and rejuvenation procedures [67] all vary the chemical components. On the other hand, the chemical composition, mineral surface anisotropy, and surface modification of the aggregate phase (retouched by hydrolyzed silane coupling agent, SCA) [93,99,103,111] are the main research points for exploring the effects of aggregate property on the interfacial bonding of bitumen-aggregate systems. Furthermore, considering the service environment, the influence of temperature [92,94,95,108,109,110,112,104–106], moisture [92,94,96,97,99], and loading rate [72,99] on the adhesion property of bitumen-aggregate interfacial systems are always investigated. Besides, some scholars considered and studied the influence of model size (bitumen film thickness) [99] and sodium chloride (NaCl) solution [113] on the adhesion parameters of bitumen-aggregate interfacial systems. The detailed influence law of these factors will be summarized in the following sections 5.2 and 5.3.

### 6.1.3. Evaluation parameters

The evaluation parameters for adhesion property of bitumen-aggregate interface systems from previous literature using MD simulation are summarized here, including the validation, interfacial, dynamics, structural and mechanical parameters. The thermodynamics outputs of the bulk bitumen model always play a crucial role in verifying the reasonability of interfacial systems and simulation settings, such as the density [72,74,92,94,96,99,106,108], glass transition temperature [72,94,96,106], cohesive energy density [92,94,96,99], solubility parameter [74,92,96,99], thermal expansion coefficient [106], isothermal compressibility [104], surface free energy (work of cohesion) [92], and bulk modulus [104]. The previous section introduced these parameters regarding the MD simulation on bulk bitumen systems. Table 1 shows that the density and glass transition temperature are the commonly-used validation indicators, which are easily obtained from experimental measurements or previous reports.

Apart from the static properties, the dynamics properties (mean square distance and diffusion coefficient) can also be predicted from MD simulations on bitumen-aggregate interfacial systems [74,94,97,98,104,108–110]. The difference in bitumen molecules' dynamics and wetting behaviors on the aggregate surface could be observed. At the same time, the structural characteristics are also essential to assessing the interaction mechanism between the bitumen and aggregate molecules. According to the results of the radial distribution function [74,94,96,97,103], relative concentration [74,94,96,97,105] and radius of gyration [114,115] are applied to describe the distribution of bitumen molecules on the aggregate surface. The corresponding definition and calculation steps are the same as those in bulk systems.

The evaluation parameters in bitumen-aggregate systems are proposed according to the interfacial energy theory [92,94,103] without external force. The interaction energy (or interfacial energy, adhesion energy, binding energy) is proposed to quantitatively assess the bonding strength between bitumen and aggregate molecules, which is defined as the energy difference between the sum of bulk models (bitumen and aggregate) and the whole bitumen-aggregate interfacial model [98,102,103,108,110]. Meanwhile, the work of adhesion (or adhesion energy, interfacial work) is another intuitive index to characterize the adhesion work of bitumen-aggregate, which refers to the interfacial energy per unit area [92,94,96,97,102,103,116]. When the moisture influence is

considered, the bitumen-aggregate bi-layers interfacial model changes to the bitumen-moisture-aggregate tri-layers system. To evaluate the moisture influence on the adhesion bonding of the bitumen-aggregate interface, the energy variations of interfacial systems before and after the involvement of moisture molecules are calculated and represented as an indicator of work of debonding [92,96]. Afterward, the moisture sensitivity of adhesion performance for a bitumen-aggregate system can be characterized by the ratio of interfacial energy or work of adhesion before and after incorporating moisture molecules, which are always presented as a name of degradation ration  $R_{AD}$  or adhesion work loss rate [92]. Similarly, the influence of the bitumen phase's aging, modification, and rejuvenation on moisture damage can be measured based on the change of degradation ratio parameter.

Like the experimental pull-off test, the bitumen-aggregate interfacial molecular model was uploaded as an external tension or compression force, and the stress-separation response could be detected [72,99–101]. Afterward, the mechanical parameters of interfacial tensile strength, compression strength, elastic modulus, stress-separation curve, and maximum peak stress can be calculated to evaluate the adhesion performance between bitumen and aggregate, which can be connected with macroscale pull-off test results. Finally, it should be mentioned that the detailed information regarding the influence of material performance (bitumen and aggregate phases) and external factors (temperature, moisture, and pull-off loading rate) on the bonding properties of bitumen-aggregate interfacial systems are introduced as follows. Table 2 lists some typical cases for investigating the influence of material performance and external factors on the adhesion properties of bitumen-aggregate systems at the molecular scale.

## 6.2. Materials factors on adhesion bonding of interfacial systems

It was widely reported that the adhesion performance of the asphalt mixture was significantly influenced by bitumen and aggregate performance [139–141]. Different interfacial molecular models were established to fundamentally assess the influence at the nanoscale, and interfacial parameters outputted from MD simulations were compared.

### 6.2.1. Aggregate characteristics

Various aggregates are composed of different chemical components, which strongly affects their interaction with bitumen molecules and thus the bonding performance [142,143]. In general, the chemical components of an aggregate were determined by an X-ray diffraction (XRD) test, and its main component was selected for building the corresponding molecular model of aggregate [144]. From Table 2, the common molecular models of aggregates are Quartz ( $\text{SiO}_2$ ) [93,118–124], Calcite ( $\text{CaCO}_3$ ) [93,118–122], Albite ( $\text{Na(AlSi}_3\text{O}_8)$ ) [118,120,122], and Microcline ( $\text{(KAlSi}_3\text{O}_8)$ ) [120,122]. Afterward, their bitumen-aggregate bi-layer interfacial models could be established, as shown in Fig. 12.

The adhesion performance and moisture damage resistance of bitumen-quartz and bitumen-calcite interfaces at the molecular scale were compared by Zhai and Hao [121]. It was found that the van der Waals energy mainly contributed to the interfacial bonding between bitumen and quartz. In contrast, electrostatic energy played a dominant role in determining the adhesive property of a bitumen-calcite system. Meanwhile, the calcite aggregate exhibited a stronger moisture damage resistance than the quartz regardless of the bitumen components. The influence of aggregate components on the adhesion performance of the bitumen-aggregate interface was more significant than the bitumen property. From the study of Chu et al. [93], the aggregate type and mineral surface anisotropy remarkably affected the adhesion property of bitumen-aggregate models. They found that alkaline limestone

**Table 2**  
Typical cases for investigation on the influence of material performance and external factors on bitumen-aggregate interfacial systems.

Main factor	Bitumen model	Aggregate model	Other factors	Evaluation parameters	Ref
<b>I. Aggregate characteristics</b>	AAA-1 12-component bitumen model;	<b>a.</b> Calcite ( $\text{CaCO}_3$ , {018}, {104}); <b>b.</b> Quartz ( $\text{SiO}_2$ , {001}, {101}); <b>c.</b> Albite ( $\text{NaAlSi}_3\text{O}_8$ , {001}, {010});	(a) Moisture film thickness: 5, 10 Å;	<b>Interfacial:</b> Interfacial energy; Interfacial work; Work of debonding;	[118]
	Three-component model;	<b>a.</b> Aluminum oxide ( $\text{Al}_2\text{O}_3$ ); <b>b.</b> Calcium carbonate ( $\text{CaCO}_3$ ); <b>c.</b> Silica ( $\text{SiO}_2$ );	(a) Hydrolyzed Silane Coupling agent (SCA);	<b>Structural:</b> Radial distribution function; Relative concentration;	[119]
	Four-component bitumen model;	<b>a.</b> a-quartz ( $\text{SiO}_2$ , {001}, {100}, {101}); <b>b.</b> Calcite ( $\text{CaCO}_3$ , {104}, {214}, {018});	(a) Geometry size;	<b>Interfacial:</b> Adhesion energy;	[93]
	AAA-1 12-component bitumen model;	<b>a.</b> Quartz ( $\text{SiO}_2$ ); <b>b.</b> Alkalifeldspar ( $\text{NaAlSi}_3\text{O}_8$ ); <b>c.</b> Plagioclase ( $\text{CaAl}_2\text{SiO}_8$ ); <b>d.</b> Calcite ( $\text{CaCO}_3$ ); <b>e.</b> Mica ( $\text{NaAl}_2\text{Si}_4\text{O}_{12}$ ); <b>f.</b> MMT ( $\text{CaAl}_2\text{Si}_4\text{O}_{12}$ ); <b>g.</b> Chlorite ( $\text{Mg}_3\text{Al}_2\text{Si}_4\text{O}_{18}$ ); <b>h.</b> Nepheline ((Na, K) $\text{AlSiO}_4$ ); <b>i.</b> Pyroxene ( $\text{FeMgSi}_2\text{O}_6$ ); <b>j.</b> Olivine ( $\text{CaMgSiO}_4$ );	(a) Moisture;	<b>Validation:</b> Density; Glass transition temperature;	[120]
	AAA-1 12-component bitumen model;	<b>a.</b> Quartz ( $\text{SiO}_2$ ); <b>b.</b> Calcite ( $\text{CaCO}_3$ );	(a) Bitumen aging;	<b>Interfacial:</b> Work of adhesion; Adhesion energy; Adhesion work in wet condition; Adhesion work loss rate;	[121]
	AAA-1 12-component bitumen model;	<b>a.</b> Quartz ( $\text{SiO}_2$ ); <b>b.</b> Calcite ( $\text{CaCO}_3$ ); <b>c.</b> Albite ( $\text{NaAlSi}_3\text{O}_8$ );	(b) Moisture;	<b>Interfacial:</b> Work of adhesion; Interaction energy;	[122]
	12-component bitumen model;	<b>d.</b> Microcline ( $\text{KAlSi}_3\text{O}_8$ ); <b>a.</b> $\text{SiO}_2$ ; <b>b.</b> $\text{SiO}_2$ -SCAs;	(a) Moisture;	<b>Interfacial:</b> Work of adhesion; Interaction energy; Degradation ratio $R_{AD}$ ; Work of debonding;	[123]
	12-component bitumen;	<b>a.</b> $\text{SiO}_2$ ; <b>b.</b> $\text{CaCO}_3$ ; <b>c.</b> $\text{SiO}_2$ -SCA; <b>d.</b> $\text{CaCO}_3$ -SCA;	(a) Silane-hydrolysate coupling agents;	<b>Validation:</b> Density; Cohesive energy density; Glass transition temperature;	[124]
	<b>a.</b> 12-component virgin bitumen model; <b>b.</b> Lightly-oxidized bitumen model; <b>c.</b> Heavy-oxidized bitumen model;	Quartz ( $\text{SiO}_2$ ); Calcite ( $\text{CaCO}_3$ ); Albite ( $\text{NaAlSi}_3\text{O}_8$ ); Microcline ( $\text{KAlSi}_3\text{O}_8$ );	(b) Moisture;	<b>Interfacial:</b> Interaction energy; Energy ratio; <b>Structural:</b> Concentration profile; Radial distribution function; Transition zone range; Contact angle; Hydrogen bond analysis;	[111]
	<b>a.</b> Four component virgin bitumen; <b>b.</b> 0–20 h short-term aged bitumen; <b>c.</b> PAV long-term aged bitumen;	$\text{Al}_2\text{O}_3$ ; $\text{SiO}_2$ ; $\text{CaO}$ ;	(a) Moisture;	<b>Validation:</b> Density; Radial distribution function; Cohesive energy density; Solubility parameter;	[125]
<b>II. Bitumen properties</b>	<b>a.</b> 12-component virgin bitumen; <b>b.</b> Short-term aged bitumen; <b>c.</b> Long-term aged bitumen; <b>d.</b> Silica cluster modified bitumen;	Silica regularity model; Silica irregularity model with the radius of 0.5 nm and 1.0 nm;	(b) Moisture;	<b>Interfacial:</b> Adhesion energy; Adhesion degradation rate; Debonding energy;	[126]
	<b>a.</b> Four-component virgin bitumen; <b>b.</b> Carbon nanotube modified bitumen; <b>c.</b> Graphene modified bitumen;	$\text{SiO}_2$	(a) Moisture;	<b>Interfacial:</b> Work of adhesion at dry and wet conditions; Interaction energy;	[111]
	<b>a.</b> AAA-1 12-component virgin bitumen; <b>b.</b> Bis(2-hydroxyethyl) terephthalate modified bitumen;	$\alpha$ - $\text{SiO}_2$ ; $\beta$ - $\text{SiO}_2$	(a) Moisture;	<b>Validation:</b> Density; Cohesive energy density; <b>Structural:</b> Fraction of free volume; Radial distribution function;	[112]
	<b>a.</b> AAA-1 12-component virgin bitumen; <b>b.</b> Algae bio-bitumen <b>c.</b> SBS modified bitumen;	$\text{SiO}_2$ ;	(a) Temperature: –12–16 °C;	<b>Validation:</b> Density; Cohesive energy density; <b>Structural:</b> Mean square distance; <b>Mechanical:</b> Interfacial tensile strength; Compression strength; Elastic modulus;	[127]
			(a) Temperature: –12–16 °C;	<b>Interfacial:</b> Adhesion work; <b>Validation:</b> Cohesive energy density;	[128]

(continued on next page)



Table 2 (continued)

Main factor	Bitumen model	Aggregate model	Other factors	Evaluation parameters	Ref
Moisture damage	a. AAA-1 12-component virgin bitumen; b. Aged bitumen; c. Rejuvenated bitumen;	SiO <sub>2</sub> ; Al <sub>2</sub> O <sub>3</sub> ;	(a) Moisture; (b) Rejuvenator content; (c) Temperature;	<b>Validation:</b> Surface free energy; <b>Interfacial:</b> Adhesion work; Debonding work; Energy ratio; The percentage of decrease in the work of adhesion;	[67]
	a. NY1 12-component virgin bitumen; b. NY3 aged bitumen; c. Waste cooking oil rejuvenated bitumen;	SiO <sub>2</sub> ; CaO; MgO; CaCO <sub>3</sub> ;	(a) Moisture; (b) Rejuvenator content;	<b>Validation:</b> Density; Surface free energy; Solubility parameter; <b>Interfacial:</b> Work of adhesion; Work of debonding; Energy ratio; Degradation ratio;	[91]
	AAA-1 12-component bitumen;	$\alpha$ -SiO <sub>2</sub> ; CaCO <sub>3</sub> ; Na <sub>2</sub> O·Al <sub>2</sub> O <sub>3</sub> ·6SiO <sub>2</sub>		<b>Validation:</b> Density; Cohesive energy density; Solubility parameter; Glass transition temperature; <b>Structural:</b> Radial distribution function; Relative concentration; <b>Interfacial:</b> Interfacial adhesion energy; Debonding energy;	[129] [130]
	AAA-1 12-component bitumen; (Virgin and aged)	Quartz (SiO <sub>2</sub> ); Calcite (CaCO <sub>3</sub> );	(a) Moisture layers of 100, 150, and 200 water molecules;	<b>Validation:</b> Density; <b>Structural:</b> Radial distribution function; Relative concentration;	[131]
	AAA-1 12-component bitumen;	Silica (SiO <sub>2</sub> ) (001), (101); Calcite (CaCO <sub>3</sub> ) (104), (018), (214);	(a) Mineral surface anisotropy;	<b>Interfacial:</b> Adhesion energy; Energy ratio; <b>Interfacial:</b> Adhesion energy; Wetting process (Contact angle); Work of debonding; Improved energy ratio; Hydrogen bond interaction;	[132]
	Three-component bitumen;	Quart (SiO <sub>2</sub> );	(a) Moisture dosage: 0, 0.5, 1.0, 1.5 %; (b) Atomistic model size (number of atoms); (c) Loading rate: 5.0E9, 1.0E9, 1.0E8, 1.0E8 1/s; (d) Temperatures: −35, −5, 25, 85, 170 °C;	<b>Interfacial:</b> Stress-separation curve; Maximum interface stress; <b>Validation:</b> Density; Thermal expansion coefficient; Isothermal compressibility; Bulk modulus;	[133]
	12-component bitumen;	–	(a) Oxidation aging; (b) Moisture content: 0, 2.5 %, 5.0 %, 7.5 %, 10.0 %;	<b>Validation:</b> Density; Bulk modulus; Zero shear viscosity;	[134]
	Four-component bitumen;	–	(a) Aging stages: original, Mid, and End-aging; (b) Moisture layer;	<b>Interfacial:</b> Interfacial energy (moisture-bitumen); <b>Validation:</b> Energy; Temperature;	[135]
	Three-component bitumen;	Crystal quartz (SiO <sub>2</sub> );	(a) Nano hydrated lime (NHL); (b) Moisture; (c) Aging functional groups;	<b>Interfacial:</b> Adhesion energy;	[136]
	Three-component bitumen;	Quartz (SiO <sub>2</sub> ); Calcite (CaCO <sub>3</sub> ); Albite (NaAlSi <sub>3</sub> O <sub>8</sub> ); Microcline (KAlSi <sub>3</sub> O <sub>8</sub> );		<b>Interfacial:</b> Work of adhesion; Degradation ratio (R <sub>AD</sub> ); Work of debonding;	[137]
	12-component bitumen;	Microcline (KAlSi <sub>3</sub> O <sub>8</sub> ); Quartz (SiO <sub>2</sub> ); Calcite (CaCO <sub>3</sub> );	(a) Bitumen thickness; (b) Pull-off velocities; (c) Temperature;	<b>Interfacial:</b> Cohesive debonding percentage; Interface energy	[138]
	Three-component bitumen 12-component bitumen;	Quartz (SiO <sub>2</sub> ); Calcite (CaCO <sub>3</sub> ); SiO <sub>2</sub> ;	(a) Bitumen types;	<b>Structural:</b> Radius of gyration; vdW volume; <b>Structural:</b> Radius of gyration; Relative concentration;	[114] [115]

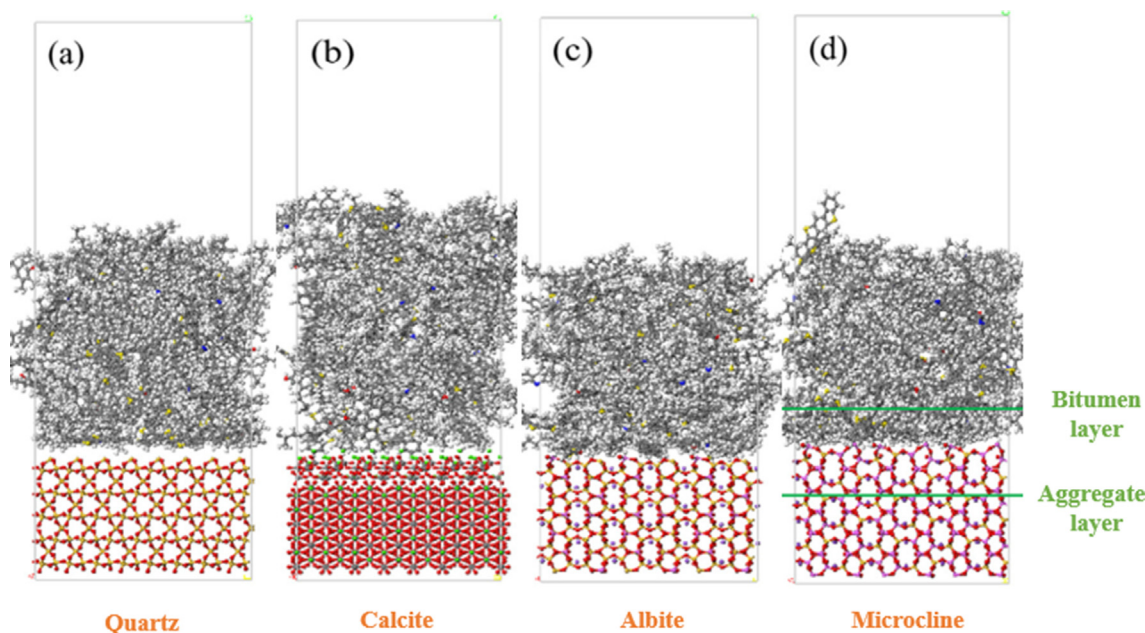


Fig. 12. Bitumen and aggregate models in different interfacial systems [122].

(calcite) showed a stronger bonding strength with bitumen than acidic silica (quartz) due to the larger hydrogen bond. In addition, they suggested that the van der Waals and electrostatic interactions were both important to the adhesion performance of the bitumen-calcite interface. Importantly, for the quartz-bitumen interface, the bonding strength ranking is  $(101) > (100) > (001)$ , while for a calcite-bitumen interface, the bonding strength ranking is  $(018) > (214) > (104)$ .

Due to the poor interfacial bonding strength of acidic aggregate (granite), Cui and Wang [123] modified the quartz mineral surface with silane coupling agents (SCA). They validated the positive role of SCA in enhancing the adhesion performance of the bitumen-quartz interface under both dry and wet conditions. In addition, the grafted SCA significantly improved the moisture damage resistance of the bitumen-quartz interface because of the enlarged interaction energy and reduced potential of hydrogen bonds. Some simulations were performed by Ding et al. [119], and the addition of SCA distinctly promoted the molecular distribution of bitumen molecules on a granite surface. Peng et al. [124] compared the different silane-hydrolysate coupling agents on interfacial bonding between bitumen and  $\text{SiO}_2$  or  $\text{CaCO}_3$ . The hydrolysate KH792 exhibited a much strong effect on adhesion enhancement than KH550. Interestingly, it was mentioned that the silane-hydrolysates increased the debonding energy between bitumen and  $\text{SiO}_2$  aggregate but decreased that for the bitumen- $\text{CaCO}_3$  interface.

Gao et al. [122] also concluded that the bonding and debonding behaviors of the bitumen-mineral interface were significantly dependent on the mineralogical characteristics and components. When the bitumen phase was the same, the ranking of adhesion bonding for different aggregates was microcline > albite > calcite > quartz in both dry and wet conditions. In addition, the moisture damage levels of the various bitumen-aggregate interface were different. The adhesion bonding strength between bitumen and quartz, calcite, albite, and microcline were reduced by 82 %, 84 %, 18 %, and 1 % after the moisture invasion. Feng et al. [118] classified the limestone, granite, and tuff into alkaline, acid, and neutral lithology group based on the  $\text{SiO}_2$  dosage. They also observed that the interfacial bonding level of the bitumen-aggregate system was affected by the aggregate sur-

face texture. In addition, the bitumen-calcite interface exhibited a more muscular bonding strength than granite and tuff under similar aggregate surface texture conditions. Fan et al. [120] systematically performed a coupled MD simulation and experimental study on the influence of aggregate mineralogical genome on bitumen-aggregate interfacial behaviors. Experimental results revealed that the diabase presented the best moisture damage resistance, followed by greywacke I, basalt, and greywacke II, while two granite aggregates had the highest moisture susceptibility. More vital intermolecular interaction between bitumen and aggregate led to molecular aggregation and rotation at the near-surface region and the gradient-distribution of bitumen molecules in the direction perpendicular to the surface. Moreover, the difference in competitive adsorption between bitumen and moisture molecules at the different mineral surfaces was the underlying mechanism for the difference in moisture damage resistance of the various bitumen-aggregate interface.

#### 6.2.2. Bitumen performance

The bitumen binder plays a vital role in linking the aggregates into a whole asphalt mixture, and the variation of bitumen components significantly affects the adhesion performance of the bitumen-aggregate interface. In this section, some cases are discussed and summarized to show the effects of aging, modification, and rejuvenation of bitumen on the interfacial bonding of bitumen-aggregate bi-layers molecular model predicted from MD simulations. Gao et al. [111] investigated the aging degree of bitumen on interfacial bonding of different bitumen-aggregate systems. For the bitumen-quartz, the oxidation aging of bitumen reduced its adhesion work by increasing the intermolecular distance between bitumen and quartz phases. However, the interfacial bonding of both bitumen-albite and bitumen-microcline models enlarged when bitumen molecules were oxidized, which was related to increased electrostatic energy due to high polarity. Moreover, van der Waals and electrostatic energies contributed to the bitumen-calcite system's interfacial adhesion, which decreased and increased after light and heavy oxidation aging. The reason was associated with the increased bitumen-calcite distance and enhanced polarity. Likewise, Zhang et al. [215] measured the interfacial energy and tensile strength of bitumen-

aggregate models under the tensile conditions considering the influence of bitumen aging and aggregate type. The results revealed that the micro-mechanical response and indentation characteristics of asphalt mixtures were strongly weakened as an increment in the aging level of bitumen, which showed different trends in various aggregates. It was concluded that the aging degree of bitumen was a detrimental factor to the adhesive bonding of the bitumen-aggregate interface, which had less influence on a bitumen- $\text{Al}_2\text{O}_3$  interface.

The involvement of various modifiers also changes the adhesive performance between bitumen and aggregates. Long et al. [126] compared the difference in adhesive bonding of the bitumen-silica interface before and after adding nano-silica in the bitumen phase. The existence of nano-silica could promote the asphaltene dispersion on the surface of silica aggregate and enhance the work of adhesion because of its surface effect. Although the water and sodium chloride solution condition effectively deteriorated the adhesive strength of the bitumen-silica interface, the nano-silica exhibited a positive role in reducing the moisture sensitivity of the interfacial model. Chen et al. [112] employed the MD simulations to validate the negative effect of bio-oil on the interfacial bonding of the bitumen-mineral system, which was due to the decreased diffusive capacity of bitumen molecules on the mineral surface after adding bio-oil organisms.

On the contrary, Zhang et al. [128] observed that the incorporation of bis (2-hydroxyethyl terephthalate) (BHET) modifier could significantly enhance the bonding strength of the bitumen-granite interface due to its high polarity. Meanwhile, the moisture damage resistance of the bitumen-granite interface was increased by 42 % after adding the BHET modifier, which significantly enlarged the hydrophobic characteristics of bitumen. The van der Waals energy played a dominant role in determining the interaction force between bitumen and granite. The addition of BHET increased hydrogen bonding energy, much stronger than the van der Waals term.

The restoration capacity of rejuvenators on the adhesion performance of the bitumen-aggregate interface was studied by MD simulations. Cui et al. [67] observed that for both  $\text{Al}_2\text{O}_3$  than  $\text{SiO}_2$  aggregates, the work of adhesion and work of debonding for aged bitumen presented an upward trend with an increment in rejuvenator dosage, and the positive influence of rejuvenator on adhesive bonding and moisture damage resistance was more significant on  $\text{Al}_2\text{O}_3$  than  $\text{SiO}_2$ . Similarly, Yan et al. [91] examined the role of waste cooking oil (WCO) in regenerating the adhesion performance of aged bitumen-aggregate systems with four types of aggregates: basalt ( $\text{SiO}_2$ ), limestone ( $\text{MgO}$ ), granite ( $\text{CaCO}_3$ ), and sandstone ( $\text{CaO}$ ). The surface free energy (SFE) parameters of these interfacial systems were calculated based on contact angle measurement, and the adhesion work could be derived. At the same time, the MD simulations were conducted on these interfacial models to evaluate the influence of WCO on adhesion performance at the molecular level. It was found that the SFE parameters and adhesion work of aged bitumen to aggregates were remarkably improved by adding WCO, but the rejuvenation effect showed a decreasing trend with an increment of WCO dosage. Meanwhile, the rejuvenation influence of WCO on the adhesion property of aged bitumen-aggregate models was strongly dependent on aggregate components. In addition to the  $\text{SiO}_2$ ,  $\text{MgO}$ , and  $\text{CaCO}_3$  minerals, incorporating a WCO rejuvenator could increase adhesion work and moisture damage resistance of the corresponding interfacial systems, which displayed an opposite influence on the bitumen- $\text{CaO}$  system. Lastly, the SFE parameters, adhesion work, and moisture damage resistance of the aged bitumen-aggregate interface could be restored to the virgin bitumen level when the WCO dosage was 4–6 wt%.

### 6.3. External factors for adhesion bonding of interfacial systems

Apart from material performance, environmental factors also play a vital role in affecting the interfacial bonding of the asphalt mixture. The common external factors in MD simulations on bitumen-aggregate interfacial systems contain moisture invasion, temperature variation, and pull-off loading rate.

#### 6.3.1. Moisture invasion

Due to the difference in the hydrophilic and hydrophobic characteristics of aggregate and bitumen, the interfacial bonding of the bitumen-aggregate system would be strongly influenced by the moisture invasion. The moisture could occupy and replace the bitumen on the aggregate surface, and the interfacial debonding phenomenon would occur. From macroscale tests, the tensile strength of the asphalt mixture would reduce significantly after immersing in a water environment for a while. Fig. 13 illustrates the molecular-level mechanism of moisture invasion on a bitumen-aggregate interface.

Cui et al. [129,130] investigated the influence of moisture on the adhesion performance of bitumen-silica (granite) and bitumen-calcite (limestone) interfacial systems. Based on relative concentration and radial distribution function results, it was observed that the moisture invasion reduced the concentration distribution of bitumen molecules on the aggregate surface and changed the nanostructure of the bitumen-aggregate surface. Thus, the adhesion energy between bitumen and aggregate was weakened. For the bitumen-silica system, the absorbed moisture molecules slightly reduced its water damage resistance, negatively weakening the adhesion performance of the bitumen-calcite interfacial model. Furthermore, it was explained that the  $\text{CO}_3^{2-}$  and  $\text{Ca}^{2+}$  ions in calcite (limestone) aggregate were prone to necking of electron density, and the  $\text{CO}_3^{2-}$  ions could easily form bonds with  $\text{H}^+$  ions in residual absorbed water to form  $\text{HCO}_3^-$ .

Sun and Wang [131] employed MD simulation to estimate the moisture influence on the molecular interaction between bitumen with silica and calcite aggregates considering the aging factor. As expected, the incorporation of the molecular moisture layer remarkably reduced the interfacial bonding property of the bitumen-aggregate interface regardless of the aggregate component. Moreover, it was interesting to find that the influence of moisture on the adhesion energy of SARA fractions differed from each other and the whole system. Compared to the bitumen-silica system, the bitumen-calcite interface exhibited a more substantial adhesion capacity but more considerable moisture sensitivity. In addition, they also observed that the existence of moisture molecules changed the self-agglomeration potential of asphaltene molecules and the molecular distribution level of SARA components, which significantly affected the adhesive bonding degree of the bitumen-aggregate interface. Lastly, the moisture sensitivity of the bitumen-aggregate system would depend on the bitumen components (ratio of SARA fractions) and the corresponding nanostructure.

Luo et al. [132] conducted the MD simulations on wetting performance and moisture damage resistance of bitumen-quartz and bitumen-calcite interfaces from the aspect of the shape and anisotropic characteristic of aggregate models, which were evaluated by a contact angle of water nano-droplet on anisotropic mineral surfaces and an improved energy ratio considering the residual adhesion in a moisture state. Compared to freshly cleaved quartz aggregate, the concentrated hydroxyl groups on its surface distinctly enlarged the surface hydrophilicity and weakened the moisture resistance of the bitumen-quartz interfacial system. On the other hand, the contact angle of the moisture droplet on the freshly-cleaved calcite surface was much larger than that on the quartz surface, which indicated that the freshly-cleaved calcite



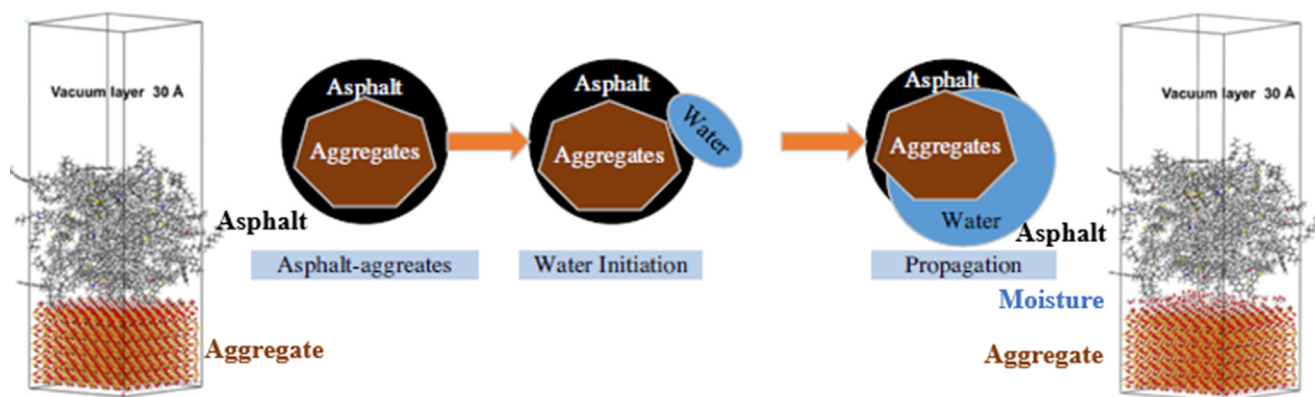


Fig. 13. Moisture invasion on the bitumen-aggregate interface [117,123,136].

aggregate exhibited a more vital interaction with moisture molecules. Gong et al. [137] explored the moisture sensitivity of the bitumen-quartz interface with MD simulations considering the influence of bitumen characteristics and temperature. It was reported that the degradation of adhesion bonding level was more significant when the temperature exceeded the softening point of bitumen. The high-and-low temperatures cyclic process would accelerate the moisture damage and interfacial cracking of the bitumen-aggregate system, which was validated by an AFM test. Moreover, the bitumen-quartz interface containing a stiffer bitumen exhibited a higher moisture sensitivity, and the influence of bitumen characteristics was negligible at high temperatures.

### 6.3.2. Temperature variation

The system temperature remarkably influences the thermodynamic and interfacial properties of a bitumen-aggregate model. Most of the studies concentrated on the molecular interaction and adhesion behaviors of bitumen-aggregate systems considering the influence of temperature. For example, Xu and Wang [92] evaluated the stress-separation curves of bitumen-silica interfacial models at temperatures of  $-30$ ,  $0$ ,  $25$ ,  $80$ , and  $135$  °C. The results revealed that the interfacial failure strength presented a decreasing trend with a significantly increasing temperature. It was consistent with the experimental result from pull-off tests. The molecular mobility of bitumen molecules near the aggregate surface enlarged at high temperatures, which increased the breaking potential and decreased the energy required to separate the bitumen molecules from the aggregate surface. The same conclusion was drawn by Chen et al. [112], reporting that the interfacial energy between the silica aggregate and various algae bio-bitumen molecules reduced progressively as the temperature rose from  $-15$  to  $15$  °C.

In addition, the low temperature region of  $-35$ – $0$  °C with an interval of  $10$  °C was selected by Zheng et al. [108] to explore the microscopic adhesion performance of the bitumen-aggregate interface in cold areas. Although the influence of temperature on interaction energy between bitumen components and the silica phase was not evident, it was found that the aromatic and saturate dosage significantly influenced the molecular-level adhesion properties of the bitumen-aggregate interface at low temperatures. In the meantime, asphaltene played a minor role in determining the low-temperature interfacial adhesion property. Liu et al. [97] investigated the interfacial adhesion performance of bitumen-steel slag interface systems with MD simulations considering the influence of bitumen components, temperature, and moisture content. The adhesion work of the bitumen-steel slag interface at variable temperatures of  $-20$ ,  $0$ ,  $25$ ,  $60$ , and  $80$  °C was measured. It suggested that the interfacial bonding strength between bitumen and steel slag was negatively related to the increased temperature,

significantly reduced with the highest trend when the temperature was close to the softening point of bitumen. Meanwhile, SARA fractions exhibited different adhesion behaviors on the steel-slag surface, and highly-polar molecules (resin and asphaltene) showed a higher diffusive capacity near steel slag, but the asphaltene molecules displayed enormous sensitivity to variation in temperature and humidity. Lastly, it was explained that the underlying mechanism regarding the coupling effects of temperature and moisture on atomic-scale interfacial adhesion of bitumen-steel slag came from the variation of self-agglomeration of asphaltene molecules and colloidal structure of the whole bitumen model. Gong et al. [137] also assessed the coupling influence of moisture and temperature on bitumen-aggregate interfacial systems. They mentioned that the debonding effect of moisture was more apparent when the temperature exceeded the softening point, and the multi-cycling temperature dramatically reduced the interfacial adhesion capacity of the bitumen-aggregate surface.

### 6.3.3. Pull-off loading rate

The bitumen-aggregate interfacial molecular model was also subjected to the pull-off procedure to directly connect the MD simulation outputs with macroscale experimental adhesion parameters. As shown in Fig. 14a, the aggregate phase was fixed, and bitumen molecules in a thin top layer were given a vertical moving speed of  $V_0$ . Afterward, the failure type at the molecular level of the bitumen-aggregate interface could be observed. The corresponding pull-off strength would be obtained based on the stress-separation curve by tracing the atomic force during the pull-off process. As expected, the loading rate plays a crucial role in affecting the failure type and bonding performance of the bitumen-aggregate interfacial system. Du et al. [99] systematically elucidated the impact of tensile rate on the deformation behavior and bonding parameter of a bitumen-silica molecular interface. The configuration results are illustrated in Fig. 14b. The interfacial deformation type strongly depended on the pull-off loading rate, which changes from fully-adhesion failure to adhesion-cohesion failure till fully-cohesion damage with the tensile rate decreased from  $1 \times 10^{-2}$  to  $5 \times 10^{-3}$  and less than  $1 \times 10^{-3}$  Å/fs, respectively. This finding is hardly observed but measured by a macroscale pull-off experiment on the basis of a significant discrepancy in BBS value. Interestingly, the predicted interfacial strength of the adhesion failure was about five times that of cohesion damage.

Similarly, Wang et al. [133] conducted the pull-off MD simulation on a bitumen-aggregate interfacial model considering the influence of bitumen components, atomic model size, pull-off loading rate, temperature, and moisture. The interface stress-separation curve of the bitumen-aggregate molecular model was drawn during the tensile process, displayed in Fig. 14c. As the dis-

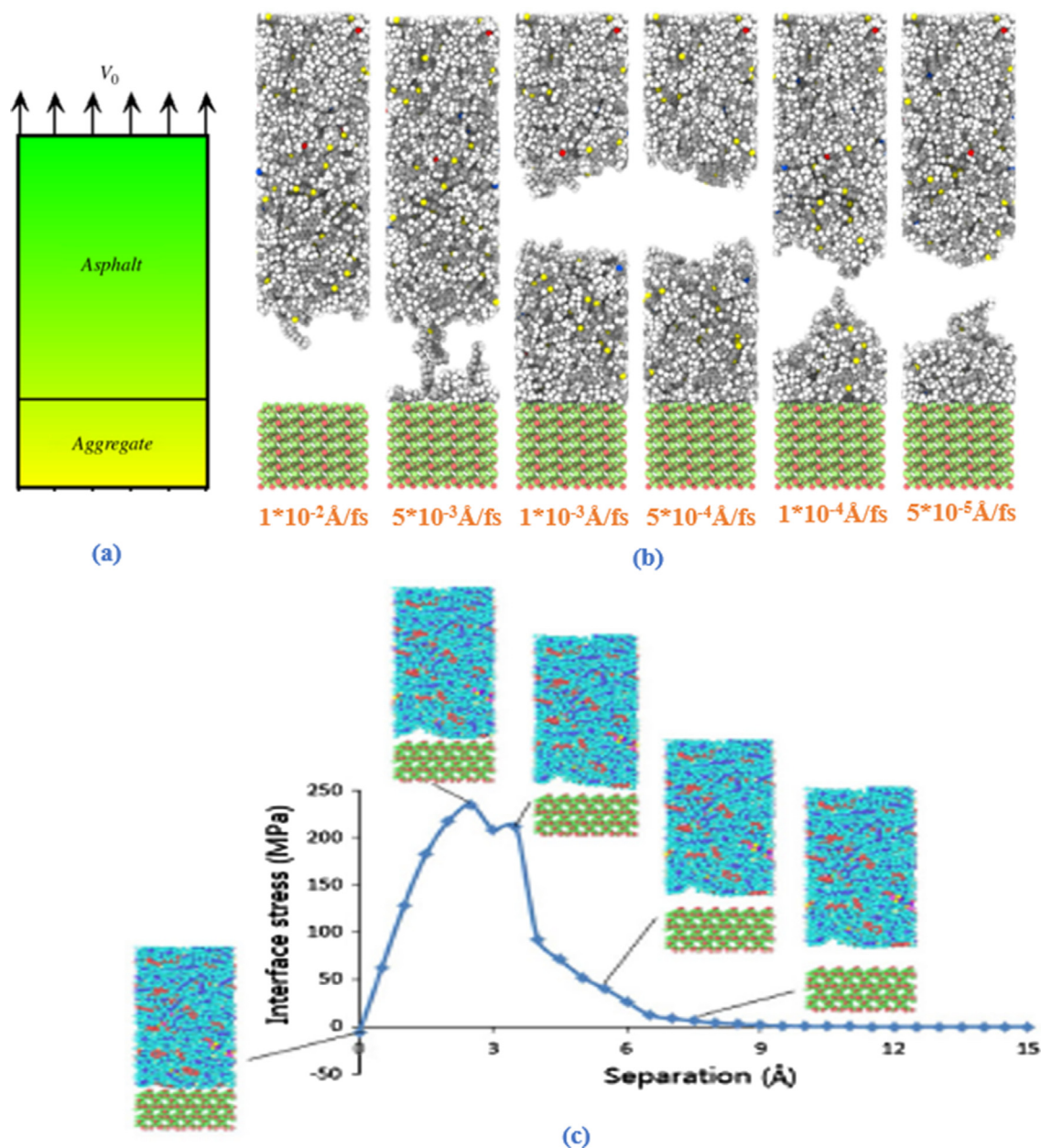


Fig. 14. Typical MD prediction of interface tensile stress at a bitumen-aggregate interface [99,133].

tance between bitumen and aggregate phases increased, the interface stress rose to a peak value and then dropped down to zero gradually, which presented the same trend as the experimental pull-off curve. In addition, it proved that the role of loading rate on the predicted adhesive bonding strength of the bitumen-quartz interface could not be ignored. Meanwhile, the effects of increased moisture dosage and temperature on weakening the interface adhesion performance were also observed.

Lu and Wang [198] found that the uploaded stress level also controlled the tensile strength of the bitumen-aggregate molecular interfacial model, and a low strain rate was beneficial to enlarging the flexibility characteristic of the interfacial adhesive damage. When the pull-off loading velocity was in a specific region, cohesive and adhesive failures could co-occur. Chen et al. [138] tried to quantify the bitumen-aggregate molecular interface's cohesion and adhesion failure percentage during the pull-off simulation. The aggregate composition showed a significant influence on the

failure type of interface. In their study, all bitumen-quartz interfaces showed complete adhesive debonding, while all bitumen-microcline interfaces occurred cohesive damage. Importantly, it was found that the cohesion debonding ratio of the bitumen-calcite interface increased with the increase of temperature and decrease of loading velocity.

## 7. Conclusions and recommendations

This paper reviewed the applications of the MD simulation method in the diffusion behaviors, self-healing characteristics, and interfacial bonding performance of various multi-substance and multi-phase systems of sustainable bituminous materials. It can help us systematically understand the current functions of MD simulation in the transport and interfacial systems of bituminous materials and further develop its potential benefits in addressing the research issues in asphalt pavement engineering.

Some main conclusions and recommendations for future studies are listed as follows:

### 7.1. Main conclusions

The transport process and diffusion parameters of oxygen, moisture, and rejuvenator molecules in the bitumen matrix could be displayed and predicted from MD simulations. In addition, the molecular mobility and distribution of various bitumen molecules on the surface of the aggregate phase could be quantitatively evaluated and compared, which strongly affected the adhesion performance of the bitumen-aggregate interfacial system. The MD simulation outputs exhibit a similar trend to experimental results on the influence of temperature, pressure, bitumen components, aging, and rejuvenation on the diffusion capacity of these molecules in the bitumen matrix.

Combining MD simulations with macroscale experimental characterizations, the molecular mobility and intermolecular interaction of bitumen molecules in different layers determine the self-healing rate and ratio, respectively. Moreover, the self-healing behaviors of the SARA fractions in bitumen are significantly different, which are enhanced with the increment in temperature and the incorporation of healing agents. However, the tensile strength of damaged bitumen may not be fully recovered when the crack disappears, and the healing ratio strongly depends on the initial damage degree (crack width) and temperature.

The MD simulation is an efficient method to qualitatively and quantitatively evaluate the interfacial bonding level between bitumen and aggregate based on the intermolecular interaction energy. Moreover, the molecular-scale adhesion mechanism between bitumen and aggregate has been explained through different thermodynamics and structural parameters. In addition, the MD simulation outputs regarding the influence of bitumen characteristics, aggregate components and surface texture, temperature, moisture, and pull-off loading rate on interfacial bonding and debonding capacity of bitumen-aggregate models agree well with macroscale experimental results.

### 7.2. Recommendations for future works

More realistic molecular models of virgin and aged bitumen, rejuvenators, and aggregates should be further developed based on their chemical characteristics to ensure the sufficient reasonability of MD simulation outputs.

The macroscale experimental results should systematically validate the molecular-level diffusion, self-healing, and interfacial parameters of bituminous materials predicted from MD simulations.

The potential connections between the outputted parameters from MD simulations and macroscale properties from experiments should be explored. MD simulation will be crucial in predicting bituminous materials' transport and interfacial properties without doing large amounts of laboratory tests.

It is worth investigating the self- or mutual-diffusion behaviors of moisture, oxygen, and rejuvenator in bituminous materials under different conditions, and it is of significance to design more efficient anti-stripping, anti-aging agents, and rejuvenators.

The synergistic effects of aggregate type, temperature, aging, rejuvenation, and moisture invasion on the interfacial bonding behaviors of bitumen-aggregate models should be further explored regarding the adhesion system.

### CRediT authorship contribution statement

**Shisong Ren:** Methodology, Investigation, Formal analysis, Writing – original draft, Writing – review & editing. **Xueyan Liu:** Supervision, Writing – review & editing. **Peng Lin:** Resources,

Methodology, Supervision. **Yangming Gao:** Methodology, Supervision. **Sandra Erkens:** Methodology, Supervision.

### Declaration of Competing Interest

The authors declare that they have no known competing financial interests or personal relationships that could have appeared to influence the work reported in this paper.

### Acknowledgments

The first author would thank China Scholarship Council for the funding support (CSC, No., CSC201901530025).

### References

- [1] J. Su, E. Schlagen, Y. Wang, Investigation the self-healing mechanism of aged bitumen using microcapsules containing rejuvenator, *Constr. Build. Mater.* 85 (2015) 49–56.
- [2] S. Sobhi, S. Hesami, M. Poursoltani, P. Ayar, R.S. Mullaipudi, Coupled effects of gilsonite and sasobit on binder properties: rheological and chemical analysis, *J. Mater. Civil Eng.* 34 (3) (2022) 04021470.
- [3] Y. He, Z. Alavi, J. Harvey, D. Jones, Evaluating diffusion and aging mechanisms in blending of new and age-hardened binders during mixing and paving, *Transport. Res. Rec.: J. Transport. Res. Board* 2574 (2016) 64–73.
- [4] M. Wu, G. Xu, Y. Luan, Y. Zhu, T. Ma, W. Zhang, Molecular dynamics simulation on cohesion and adhesion properties of the emulsified cold recycled mixtures, *Constr. Build. Mater.* 333 (2022) 127403.
- [5] B. Asadi, N. Tabatabaee, Alteration of initial and residual healing potential of asphalt binders due to aging, rejuvenation, and polymer modification, *Road Mater. Pavement Des.* 23 (2) (2022) 287–307.
- [6] W.S. Mogawer, A. Booshehrian, S. Vahidi, A.J. Austerman, Evaluating the effect of rejuvenators on the degree of blending and performance of high RAP, RAS, and RAP/RAS mixtures, *Road Mater. Pavement Des.* 14 (S2) (2013) 193–213.
- [7] S. Ren, X. Liu, S. Erkens, P. Lin, Y. Gao, Multi-component analysis, molecular model construction, and thermodynamics performance prediction on various rejuvenators of aged bitumen, *J. Mol. Liq.* 360 (2022) 119463.
- [8] G. Sun, B. Li, D. Sun, J. Zhang, C. Wang, X. Zhu, Roles of aging and bio-oil regeneration on self-healing evolution behavior of asphalts within wide temperature range, *J. Cleaner Prod.* 329 (2021) 129712.
- [9] P. Ayar, F. Moreno-Navarro, M.C. Rubio-Gamez, The healing capacity of asphalt pavements: a state of the art review, *J. Cleaner Prod.* 113 (2016) 28–40.
- [10] M.D. Nazzal, W. Mogawer, A. Austerman, L.A. Qtaish, S. Kaya, Multi-scale evaluation of the effect of rejuvenators on the performance of high RAP content mixtures, *Constr. Build. Mater.* 101 (2015) 50–56.
- [11] M. Oreskovic, G.M. Pires, S. Bressi, K. Vasconcelos, D.L. Presti, Quantitative assessment of the parameters linked to the blending between reclaimed asphalt binder and recycling agent: A literature review, *Constr. Build. Mater.* 234 (2020) 117323.
- [12] F. Wang, Y. Xiao, Z. Chen, P. Cui, J. Liu, N. Wang, Morphological characteristics of mineral filler and their influence on active adhesion between aggregates and bitumen, *Constr. Build. Mater.* 323 (2022) 126520.
- [13] Q. Guo, G. Li, Y. Gao, K. Wang, Z. Dong, F. Liu, H. Zhu, Experimental investigation on bonding property of asphalt-aggregate interface under the actions of salt immersion and freeze-thaw cycles, *Constr. Build. Mater.* 106 (2019) 590–599.
- [14] L. Zhang, N. Long, Y. Liu, L. Wang, Cross-scale study on the influence of moisture-temperature coupling conditions on adhesive properties of rubberized asphalt and steel slag, *Constr. Build. Mater.* 332 (2022) 127401.
- [15] S. Ren, X. Liu, P. Lin, S. Erkens, Y. Gao, Chemical characterizations and molecular dynamics simulations on different rejuvenators for aged bitumen recycling, *Fuel* 324 (2022) 124550.
- [16] S. Rani, R. Ghabchi, S.A. Ali, M. Zaman, E.A. O'Rear, Moisture-induced damage potential of asphalt mixes containing polyphosphoric acid and antistripping agent, *Road Mater. Pavement Des.* (2021), <https://doi.org/10.1080/14680629.2021.2002180>.
- [17] Z. Fan, J. Lin, J. Xu, B. Hong, P. Liu, D. Wang, M. Oeser, Molecular insights into the adsorption configuration of bitumen colloidal on aggregate surface, *J. Mater. Civ. Eng.* 34 (4) (2022) 04022033.
- [18] R. Karlsson, U. Isacson, J. Ekblad, Rheological characterisation of bitumen diffusion, *J. Mater. Sci.* 42 (2007) 101–108.
- [19] J.C. Petersen, Asphalt oxidation – an overview including a new model for oxidation proposing that physicochemical factors dominate the oxidation kinetics, *Fuel Sci. Technol. Int.* 11 (1) (1993) 57–87.
- [20] R. Karlsson, U. Isacson, Bitumen rejuvenator diffusion as influenced by ageing, *Road Mater. Pavement Des.* 3 (2) (2002) 167–182.
- [21] S. Zhao, B. Huang, X. Shu, M.E. Woods, Quantitative evaluation of blending and diffusion in high RAP and RAS mixtures, *Mater. Des.* 89 (2016) 1161–1170.



- [22] B.R. Anupam, U.C. Sahoo, A.K. Chandrappa, A methodological review on self-healing asphalt pavements, *Constr. Build. Mater.* 321 (2022) 126395.
- [23] R. Varma, R. Balieu, N. Kringos, A state-of-the-art review on self-healing in asphalt materials: Mechanical testing and analysis approaches, *Constr. Build. Mater.* 310 (2021) 125197.
- [24] E. Santagata, O. Baglieri, L. Tsantilis, G. Chiappinelli, Fatigue and healing properties of nano-reinforced bituminous binders, *Int. J. Fatigue* 80 (2015) 30–39.
- [25] W.P. Van Oort, Durability of asphalt – It's aging in the Dark, *Ind. Eng. Chem.* 48 (7) (1956) 1196–1201.
- [26] S. Ren, X. Liu, P. Lin, Y. Gao, S. Erkens, Molecular dynamics simulation on bulk bitumen systems and its potential connections to macroscale performance: Review and discussion, *Fuel* 328 (2022) 125382.
- [27] P.R. Herrington, Diffusion and reaction of oxygen in bitumen films, *Fuel* 94 (2012) 86–92.
- [28] R. Han, X. Jin, C.J. Glover, Oxygen diffusivity in asphalts and mastics, *Pet. Sci. Technol.* 31 (15) (2013) 1563–1573.
- [29] D. Cheng, D.N. Little, R.L. Lytton, J.C. Holste, Moisture damage evaluation of asphalt mixtures by considering both moisture diffusion and repeated-load conditions, *Transport. Res. Rec.: J. Transport. Res. Board* 1832 (1) (2003) 42–49.
- [30] M. Chen, J. Geng, H. Chen, Y. Niu, R. Wang, W. Wu, S. Zhao, Z. Zhong, Diffusion of moisture and oxygen in bitumens using electrochemical impedance spectroscopy, *Fuel* 315 (2022) 123212.
- [31] E. Kassem, E. Masad, R. Lytton, R. Bulut, Measurements of the moisture diffusion coefficient of asphalt mixtures and its relationship to mixture composition, *Int. J. Pavement Eng.* 10 (6) (2009) 389–399.
- [32] M. Xu, Y. Zhang, Study of rejuvenators dynamic diffusion behavior into aged asphalt and its effects, *Constr. Build. Mater.* 261 (2020) 120673.
- [33] R. Karlsson, U. Isacson, Application of FTIR-ATR to characterization of bitumen rejuvenator diffusion, *J. Mater. Civ. Eng.* 15 (2) (2003) 157–165.
- [34] G. Cuciniello, N. Mallegni, M. Cappello, S. Filippi, P. Leandri, G. Polacco, M. Losa, Classification and selection of exhausted oils for rejuvenating bituminous blends, *Constr. Build. Mater.* 278 (2021) 122387.
- [35] Y. Xiao, Study the diffusion characteristics of rejuvenator oil in aged asphalt binder by image thresholding and GC-MS tracer analysis, *Constr. Build. Mater.* 249 (2020) 118782.
- [36] T. Ma, X. Huang, Y. Zhao, Y. Zhang, Evaluation of the diffusion and distribution of the rejuvenator for hot asphalt recycling, *Constr. Build. Mater.* 98 (2015) 530–536.
- [37] A. Mehrara, A. Khodaii, A review of state of the art on stripping phenomenon in asphalt concrete, *Constr. Build. Mater.* 38 (2013) 423–442.
- [38] L. Zhou, W. Huang, F. Xiao, Q. Lv, Shear adhesion evaluation of various modified asphalt binders by an innovative testing method, *Constr. Build. Mater.* 183 (2018) 253–263.
- [39] R. Xiao, P. Polaczyk, B. Huang, Measuring moisture damage of asphalt mixtures: The development of a new modified boiling test based on color image processing, *Measurement* 190 (2022) 110699.
- [40] M.O. Hamzah, B. Golchin, A. Jamshidi, E. Chailleux, Evaluation of rediset for use in warm-mix asphalt: a review of the literatures, *Int. J. Pavement Eng.* 16 (9) (2015) 809–831.
- [41] Y. Tan, M. Guo, Using surface free energy method to study the cohesion and adhesion of asphalt mastic, *Constr. Build. Mater.* 47 (2013) 254–260.
- [42] J. Wei, F. Dong, Y. Li, Y. Zhang, Relationship analysis between surface free energy and chemical composition of asphalt binder, *Constr. Build. Mater.* 71 (2014) 116–123.
- [43] M. Guo, M. Liang, Y. Jiao, Y. Tan, J. Yu, D. Luo, Effect of aging and rejuvenation on adhesion properties of modified asphalt binder based on AFM, *J. Microsc.* 1–12 (2021).
- [44] Y. Han, B. Cui, J. Tian, J. Ding, F. Ni, D. Lu, Evaluating the effects of styrene-butadiene rubber (SBR) and polyphosphoric acid (PPA) on asphalt adhesion performance, *Constr. Build. Mater.* 321 (2022) 126028.
- [45] L. Wang, L. Zhang, Y. Liu, Molecular dynamics study on the effect of mineral composition on the interface interaction between rubberized asphalt and aggregate, *J. Mater. Civ. Eng.* 34 (4) (2022) 04022032.
- [46] S. Ren, X. Liu, P. Lin, S. Erkens, Y. Xiao, Chemo-physical characterization and molecular dynamics simulation of long-term aging behaviors of bitumen, *Constr. Build. Mater.* 302 (2021) 124437.
- [47] Z. Long, X. Tang, N. Guo, Y. Ding, W. Ma, L. You, F. Xu, Atomistic-scale investigation of self-healing mechanism in Nano-silica modified asphalt through molecular dynamics simulation, *J. Infrastruct. Preserv. Resil.* 3 (2022) 4.
- [48] Z. Chen, J. Pei, R. Li, F. Xiao, Performance characteristics of asphalt materials based on molecular dynamics simulation – A review, *Constr. Build. Mater.* 189 (2018) 695–710.
- [49] Y. Gao, Y. Zhang, C. Zhang, X. Liu, R. Jing, Quantifying oxygen diffusion in bitumen films using molecular dynamics simulations, *Constr. Build. Mater.* 331 (2022) 127325.
- [50] Z. Liu, S. Li, Y. Wang, Waste engine oil and polyphosphoric acid enhanced the sustainable self-healing of asphalt binder and its fatigue behavior, *J. Cleaner Prod.* 339 (2022) 130767.
- [51] L. Li, Y. Yang, Y. Gao, Y. Zhang, Healing characterisations of waste-derived bitumen based on crack length: Laboratory and modelling, *J. Cleaner Prod.* 316 (2021) 128269.
- [52] A.M. Hung, M. Mousavi, E.H. Fini, Implication of wax on hindering self-healing processes in bitumen, *Appl. Surf. Sci.* 523 (2020) 146449.
- [53] W. Sun, H. Wang, Molecular dynamics simulation of nano-crack formation in asphalt binder with different SARA fractions, *Molecular Simulation*. <http://doi.org/10.1080/08927022.2055011>.
- [54] W. Cui, W. Huang, H.M.Z. Hassan, X. Cai, K. Wu, Study on the interfacial contact behavior of carbon nanotubes and asphalt binders and adhesion energy of modified asphalt on aggregate surface by using molecular dynamics simulation, *Constr. Build. Mater.* 316 (2022) 125849.
- [55] G. Chen, K. Huang, M. Miao, B. Feng, O.H. Campanella, Molecular dynamics simulation for mechanism elucidation of food processing and safety: state of the art, *Compr. Rev. Food Sci. Food Saf.* 18 (2019) 243–263.
- [56] E.C. Neyts, P. Brault, Molecular dynamics simulations for plasma-surface interactions, *Plasma Processes Polym.* 14 (2017) 1600145.
- [57] M. Seyyedattar, S. Zendeheboudi, S. Butt, Invited review-Molecular dynamics simulations in reservoir analysis of offshore petroleum reserves: A systematic review of theory and applications, *Earth Sci. Rev.* 192 (2019) 194–213.
- [58] S. Ren, X. Liu, Y. Zhang, P. Lin, P. Apostolidis, S. Erkens, M. Li, J. Xu, Multi-scale characterization of lignin modified bitumen using experimental and molecular dynamics simulation methods, *Constr. Build. Mater.* 287 (2021) 123058.
- [59] J. Barrat, J. Baschnagel, A. Lyulin, Molecular dynamics simulations of glassy polymers, *Soft Matter* 6 (2010) 3430–3446.
- [60] L. Ma, A. Vareri, R. Jing, S. Erkens, Comprehensive review on the transport and reaction of oxygen and moisture towards coupled oxidative ageing and moisture damage of bitumen, *Constr. Build. Mater.* 283 (2021) 122632.
- [61] U. Muhlich, G. Pipintakos, C. Tsakalidis, Mechanism based diffusion-reaction modelling for predicting the influence of SARA composition and ageing stage on spurt completion time and diffusivity in bitumen, *Constr. Build. Mater.* 267 (2021) 120592.
- [62] Q. Liu, J. Wu, L. Xie, Z. Zhang, X. Ma, M. Oeser, Micro-scale investigation of aging gradient within bitumen film around air-binder interface, *Fuel* 286 (2021) 119404.
- [63] X. Zhou, T.B. Moghaddam, M. Chen, S. Wu, S. Adhikari, F. Wang, Z. Fan, Nano-scale analysis of moisture diffusion in asphalt-aggregate interface using molecular simulations, *Constr. Build. Mater.* 285 (2021) 122962.
- [64] Z. Du, X. Zhu, Molecular dynamics simulation to investigate the adhesion and diffusion of asphalt binder on aggregate surfaces, *Transp. Res. Rec.* 2673 (4) (2019) 500–512.
- [65] X. Zhou, Q. Huang, S. Xu, Multi-scale analysis of moisture diffusion and distribution in different types of asphalt mixtures, *Int. J. Pavement Eng.* (2020), <https://doi.org/10.1080/10298436.2020.1736295>.
- [66] G. Xu, H. Wang, Diffusion and interaction mechanism of rejuvenating agent with virgin and recycled asphalt binder: a molecular dynamics study, *Mol. Simul.* 44 (17) (2018) 1433–1443.
- [67] B. Cui, X. Gu, D. Hu, Q. Dong, A multiphysics evaluation of the rejuvenator effects on aged asphalt using molecular dynamics simulations, *J. Cleaner Prod.* 259 (2020) 120629.
- [68] W. Sun, H. Wang, Molecular dynamics simulation of diffusion coefficients between different types of rejuvenator and aged asphalt binder, *Int. J. Pavement Eng.* 21 (8) (2020) 966–976.
- [69] M. Xu, J. Yi, D. Feng, Y. Huang, Diffusion characteristics of asphalt rejuvenators based on molecular dynamics simulation, *Int. J. Pavement Eng.* 20 (5) (2019) 615–627.
- [70] Y. Ding, B. Huang, X. Shu, Y. Zhang, M.E. Woods, Use of molecular dynamics to investigate diffusion between virgin and aged asphalt binders, *Fuel* 174 (2016) 267–273.
- [71] H. Ding, H. Wang, X. Qu, A. Varveri, J. Gao, Z. You, Towards an understanding of diffusion mechanism of bio-rejuvenators in aged asphalt binder through molecular dynamics simulation, *J. Cleaner Prod.* 126977 (2021).
- [72] G. Xu, H. Wang, Study of cohesion and adhesion properties of asphalt concrete with molecular dynamics simulation, *Comput. Mater. Sci.* 112 (2016) 161–169.
- [73] M. Guo, Y. Tan, L. Wang, Y. Hou, Diffusion of asphaltene, resin, aromatic and saturate components of asphalt on mineral aggregates surface: molecular dynamics simulation, *Road Mater. Pavement Des.* 18 (3) (2017) 149–158.
- [74] M. Huang, H. Zhang, Y. Gao, L. Wang, Study of diffusion characteristics of asphalt-aggregate interface with molecular dynamics simulation, *Int. J. Pavement Eng.* 22 (3) (2021) 319–330.
- [75] X. Luo, B. Birgisson, R.L. Lytton, Kinetics of healing of asphalt mixtures, *J. Cleaner Prod.* 252 (2020) 119790.
- [76] W. Sun, H. Wang, Self-healing of asphalt binder with cohesive failure: Insights from molecular dynamics simulation, *Constr. Build. Mater.* 262 (2020) 120538.
- [77] Y. Gong, J. Xu, E. Yan, J. Cai, The self-healing performance of carbon-based nanomaterials modified asphalt binders based on molecular dynamics simulations, *Front. Mater.* 7 (2021) 595551.
- [78] D. Sun, G. Sun, X. Zhu, Q. Pang, F. Yu, T. Lin, Identification of wetting and molecular diffusion stages during self-healing process of asphalt binder via fluorescence microscope, *Constr. Build. Mater.* 132 (2017) 230–239.
- [79] D. Sun, T. Lin, X. Zhu, Y. Tian, F. Liu, Indices for self-healing performance assessments based on molecular dynamics simulation of asphalt binders, *Comput. Mater. Sci.* 114 (2016) 86–93.
- [80] A. Bhasin, R. Bommaravaram, M.L. Greenfield, D.N. Little, Use of Molecular dynamics to investigate self-healing mechanisms in asphalt binders, *J. Mater. Civ. Eng.* 23 (4) (2011) 485–492.

- [81] X. Qu, D. Wang, Y. Hou, Q. Liu, M. Oeser, L. Wang, Investigation on self-healing behavior of asphalt binder using a six-fraction molecular model, *J. Mater. Civ. Eng.* 31 (5) (2019) 04019046.
- [82] D. Sun, G. Sun, X. Zhu, F. Ye, J. Xu, Intrinsic temperature sensitive self-healing character of asphalt binders based on molecular dynamics simulations, *Fuel* 211 (2018) 609–620.
- [83] S. Shen, X. Lu, L. Liu, C. Zhang, Investigation of the influence of crack width on healing properties of asphalt binders at multi-scale levels, *Constr. Build. Mater.* 126 (2016) 197–205.
- [84] T. Yu, H. Zhang, Y. Wang, Multi-gradient analysis of temperature self-healing of asphalt nano-cracks based on molecular simulation, *Constr. Build. Mater.* 250 (2020) 118859.
- [85] B. Shu, M. Zhou, T. Yang, Y. Li, Y. Ma, K. Liu, S. Bao, D.M. Barbieri, S. Wu, The properties of different healing agents considering the micro-self-healing process of asphalt with encapsulations, *Materials* 14 (2021) 16.
- [86] L. He, G. Li, S. Lv, J. Gao, K.J. Kowalski, J. Valentin, A. Alexiadis, Self-healing behavior of asphalt system based on molecular dynamics simulation, *Constr. Build. Mater.* 254 (2020) 119225.
- [87] L. He, Y. Zhang, A. Alexiadis, A.C. Falchetto, G. Li, J. Valentin, W. Van den bergh, Y.E. Vasiliev, K.J. Kowalski, J. Grenfell, Research on the self-healing behavior of asphalt mixed with healing agents on molecular dynamics method, *Construct. Build. Mater.* 295 (2021) 123430.
- [88] Y. Tian, M. Zheng, Y. Liu, J. Zhang, S. Ma, J. Jin, Analysis of behavior and mechanism of repairing agent of microcapsule in asphalt micro crack on molecular dynamics simulation, *Constr. Build. Mater.* 305 (2021) 124791.
- [89] M. Guo, Y. Tan, L. Wang, Y. Hou, A state-of-the-art review on interfacial behavior between asphalt binder and mineral aggregate, *Front. Struct. Civ. Eng.* 12 (2) (2018) 248–259.
- [90] F. Guo, J. Pei, J. Zhang, B. Xue, G. Sun, R. Li, Study on the adhesion property between asphalt binder and aggregate: a state-of-the-art review, *Constr. Build. Mater.* 256 (2020) 119474.
- [91] S. Yan, C. Zhou, J. Ouyang, Rejuvenation effect of waste cooking oil on the adhesion characteristics of aged asphalt to aggregates, *Constr. Build. Mater.* 327 (2022) 126907.
- [92] G. Xu, H. Wang, Molecular dynamics study of interfacial mechanical behavior between asphalt binder and mineral aggregate, *Constr. Build. Mater.* 21 (2016) 246–254.
- [93] L. Chu, L. Luo, T.F. Fwa, Effects of aggregate mineral surface anisotropy on asphalt-aggregate interfacial bonding using molecular dynamics (MD) simulation, *Constr. Build. Mater.* 225 (2019) 1–12.
- [94] W. Xu, X. Qiu, S. Xiao, G. Hu, F. Wang, J. Yuan, Molecular dynamic investigations on the adhesion behaviors of asphalt mastic-aggregate interface, *Materials* 13 (2020) 5061.
- [95] H. Yao, Q. Dai, Z. You, Investigation of the asphalt-aggregate interaction using molecular dynamics, *Pet. Sci. Technol.* 35 (6) (2017) 586–593.
- [96] J. Liu, B. Yu, Q. Hong, Molecular dynamics simulation of distribution and adhesion of asphalt components on steel slag, *Constr. Build. Mater.* 255 (2020) 119332.
- [97] J. Liu, B. Yu, S. Wang, L. Li, J. Zhang, Use of tricalcium silicate to evaluate asphalt absorption on steel slag: atomic simulation and micro-scale characterization, *Measurement* 109224 (2021).
- [98] X. Zhou, G. Zhao, S. Tighe, M. Chen, S. Wu, S. Adhikari, Y. Gao, Quantitative comparison of surface and interface adhesive properties of fine aggregate asphalt mixtures composed of basalt, steel slag, and andesite, *Constr. Build. Mater.* 246 (2020) 118507.
- [99] Z. Du, X. Zhu, F. Li, S. Zhou, Z. Dai, Failure of the asphalt-aggregate interface under tensile stress: Insight from molecular dynamics, *J. Mater. Civ. Eng.* 33 (3) (2021) 04021008.
- [100] Y. Lu, L. Wang, Nano-mechanics modelling of deformation and failure behaviours at asphalt-aggregate interfaces, *Int. J. Pavement Eng.* 12 (4) (2011) 311–323.
- [101] Y. Lu, L. Wang, Nanoscale modelling of mechanical properties of asphalt-aggregate interface under tensile loading, *Int. J. Pavement Eng.* 11 (5) (2010) 393–401.
- [102] Z. Xu, Y. Wang, J. Cao, J. Chai, C. Cao, Z. Si, Y. Li, Adhesion between asphalt molecules and acid aggregates under extreme temperature: A ReaxFF reactive molecular dynamics study, *Constr. Build. Mater.* 285 (2021) 122882.
- [103] X. Ma, J. Wu, Q. Liu, W. Ren, M. Oeser, Molecular dynamics simulation of the bitumen-aggregate system and the effect of simulation details, *Constr. Build. Mater.* 285 (2021) 122886.
- [104] D. Luo, M. Guo, Y. Tan, Molecular simulation of minerals-asphalt interfacial interaction, *Minerals* 8 (2018) 176.
- [105] M. Guo, Y. Tan, J. Wei, Using molecular dynamics simulation to study concentration distribution of asphalt binder on aggregate surface, *J. Mater. Civ. Eng.* 30 (5) (2018) 04018075.
- [106] H. Dan, Z. Zou, Z. Zhang, J. Tan, Effects of aggregate type and SBS copolymer on the interfacial heat transport ability of asphalt mixture using molecular dynamics simulation, *Constr. Build. Mater.* 250 (2020) 118922.
- [107] D.D. Li, M.L. Greenfield, Chemical compositions of improved model asphalt systems for molecular simulations, *Fuel* 115 (2014) 347–356.
- [108] C. Zheng, C. Shan, J. Liu, T. Zhang, X. Yang, D. Lv, Microscopic adhesion properties of asphalt-mineral aggregate interface in cold area based on molecular simulation technology, *Constr. Build. Mater.* 121151 (2021).
- [109] B. Sun, X. Zhou, Diffusion and rheological properties of asphalt modified by bio-oil regenerant derived from waste wood, *J. Mater. Civ. Eng.* 30 (2) (2018) 04017274.
- [110] Y. Kang, D. Zhou, Q. Wu, R. Liang, S. Shangguan, Z. Liao, N. Wei, Molecular dynamics study on the glass forming process of asphalt, *Constr. Build. Mater.* 214 (2019) 430–440.
- [111] Y. Gao, Y. Zhang, Y. Yang, J. Zhang, F. Gu, Molecular dynamics investigation of interfacial adhesion between oxidised bitumen and mineral surfaces, *Appl. Surf. Sci.* 479 (2019) 449–462.
- [112] W. Chen, S. Chen, C. Zheng, Analysis of micromechanical properties of algae bio-based bio-asphalt-mineral interface based on molecular simulation technology, *Constr. Build. Mater.* 306 (2021) 124888.
- [113] Z. Long, X. Tang, Y. Ding, M. Miljkovic, A. Khanal, W. Ma, L. You, F. Xu, Influence of sea salt on the interfacial adhesion of bitumen-aggregate systems by molecular dynamics simulation, *Constr. Build. Mater.* 336 (2022) 127471.
- [114] Z. Liu, L. Cao, T. Zhou, Z. Dong, Multiscale investigation of moisture-induced structural evolution in asphalt-aggregate interfaces and analysis of the relevant chemical relationship using atomic force microscopy and molecular dynamics, *Energy Fuels* 34 (2020) 4006–4016.
- [115] Z. Dong, Z. Liu, P. Wang, X. Gong, Nanostructure characterization of asphalt-aggregate interface through molecular dynamics simulation and atomic force microscopy, *Fuel* 189 (2017) 155–163.
- [116] X. Qu, Z. Fan, T. Li, B. Hong, Y. Zhang, J. Wei, D. Wang, M. Oeser, Understanding of asphalt chemistry based on the six-fraction method, *Constr. Build. Mater.* 311 (2021) 125241.
- [117] B. Cui, X. Gu, H. Wang, D. Hu, Numerical and experimental evaluation of adhesion properties of asphalt-aggregate interfaces using molecular dynamics simulation and atomic force microscopy, *Road Mater. Pavement Des.* (2021) 1–21, <https://doi.org/10.1080/14680629.2021.1910547>.
- [118] P. Feng, H. Wang, H. Ding, J. Xiao, M. Hassan, Effects of surface texture and its mineral composition on interfacial behavior between asphalt binder and coarse aggregate, *Constr. Build. Mater.* 262 (2020) 120869.
- [119] G. Ding, X. Yu, F. Dong, Z. Ji, J. Wang, Using silane coupling agent coating on acidic aggregate surfaces to enhance the adhesion between asphalt and aggregate: a molecular dynamics simulation, *Materials* 13 (2020) 5580.
- [120] Z. Fan, J. Lin, Z. Chen, P. Liu, D. Wang, M. Oeser, Multiscale understanding of interfacial behavior between bitumen and aggregate: from the aggregate mineralogical genome aspect, *Constr. Build. Mater.* 271 (2021) 121607.
- [121] R. Zhai, P. Hao, Research on the impact of mineral type and bitumen ageing process on asphalt-mineral adhesion performance based on molecular dynamics simulation method, *Road Mater. Pavement Des.* (2020), <https://doi.org/10.1080/14680629.2020.1739119>.
- [122] Y. Gao, Y. Zhang, F. Gu, T. Xu, H. Wang, Impact of minerals and water on bitumen-mineral adhesion and debonding behaviours using molecular dynamics simulations, *Constr. Build. Mater.* 171 (2018) 214–222.
- [123] B. Cui, H. Wang, Molecular interaction of asphalt-aggregate interface modified by silane coupling agents at dry and wet conditions, *Appl. Surf. Sci.* 572 (2022) 151365.
- [124] C. Peng, L. Lu, Z. You, F. Xu, L. You, M. Miljkovic, C. Guo, S. Huang, H. Ma, Y. Hu, Y. Liu, J. Dai, J. Zhu, H. Bi, Influence of silane-hydrolysate coupling agents on bitumen-aggregate interfacial adhesion: An exploration from molecular dynamics simulation, *Int. J. Adhes. Adhes.* 102993 (2022).
- [125] X. Zhang, J. Wang, X. Zhou, Z. Zhang, X. Chen, Mechanical properties of the interfacial bond between asphalt-binder and aggregates under different aging conditions, *Materials* 14 (2021) 1221.
- [126] Z. Long, L. You, X. Tang, W. Ma, Y. Ding, F. Xu, Analysis of interfacial adhesion properties of nano-silica modified asphalt mixtures using molecular dynamics simulation, *Constr. Build. Mater.* 255 (2020) 119354.
- [127] M.G. Ramezani, J. Rickgauer, Understanding the adhesion properties of carbon nanotube, asphalt binder, and mineral aggregates at the nanoscale: a molecular dynamics study, *Pet. Sci. Technol.* 38 (1) (2020) 28–35.
- [128] H. Zhang, M. Huang, J. Hong, F. Lai, Y. Gao, Molecular dynamics study on improvement effect of bis (2-hydroxyethyl) terephthalate on adhesive properties of asphalt-aggregate interface, *Fuel* 285 (2021) 119175.
- [129] W. Cui, W. Huang, B. Hu, J. Xie, Z. Xiao, X. Cai, K. Wu, Investigation of the effects of adsorbed water on adhesion energy and nanostructure of asphalt and aggregate surfaces based on molecular dynamics simulation, *Polymers* 12 (2020) 2339.
- [130] W. Cui, W. Huang, Z. Xiao, J. Xie, B. Hu, X. Cai, K. Wu, The effect of moisture on the adhesion energy and nanostructure of asphalt-aggregate interface system using molecular dynamics simulation, *Molecules* 25 (2020) 4165.
- [131] W. Sun, H. Wang, Moisture effect on nanostructure and adhesion energy of asphalt on aggregate surface: a molecular dynamics study, *Appl. Surf. Sci.* 510 (2020) 145435.
- [132] L. Luo, L. Chu, T.F. Fwa, Molecular dynamics analysis of moisture effect on asphalt-aggregate adhesion considering anisotropic mineral surfaces, *Appl. Surf. Sci.* 527 (2020) 146830.
- [133] H. Wang, E. Lin, G. Xu, Molecular dynamics simulation of asphalt-aggregate interface adhesion strength with moisture effect, *Int. J. Pavement Eng.* 18 (5) (2017) 414–423.
- [134] J. Pan, R.A. Tarefder, M.I. Hossain, Study of moisture impact on asphalt before and after oxidation using molecular dynamics simulations, *Transport. Res. Rec.: J. Transport. Res. Board* 2574 (2016) 38–47.
- [135] T. Yu, H. Zhang, Y. Wang, Interaction of asphalt and water between porous asphalt pavement voids with different aging stage and its significance to drainage, *Constr. Build. Mater.* 252 (2020) 119085.

- [136] H. Yao, Q. Dai, Z. You, Chemo-physical analysis and molecular dynamics (MD) simulation of moisture susceptibility of nano hydrated lime modified asphalt mixtures, *Constr. Build. Mater.* 101 (2015) 536–547.
- [137] Y. Gong, J. Xu, E. Yan, Intrinsic temperature and moisture sensitive adhesion characters of asphalt-aggregate interface based on molecular dynamics simulations, *Constr. Build. Mater.* 292 (2021) 123462.
- [138] P. Chen, X. Luo, Y. Gao, Y. Zhang, Modeling percentages of cohesive and adhesive debonding in bitumen-aggregate interfaces using molecular dynamics approaches, *Appl. Surf. Sci.* 571 (2022) 151318.
- [139] X. Qu, D. Wang, L. Wang, Y. Huang, Y. Hou, M. Oeser, The state-of-the-art review on molecular dynamics simulation of asphalt binder, *Adv. Civil Eng.* (2018) 4546191.
- [140] M. Shishehbor, M.R. Pouranian, R. Imaninassb, Evaluating the adhesion properties of crude oil fractions on mineral aggregates at different temperatures through reactive molecular dynamics, *Pet. Sci. Technol.* 36 (24) (2018) 2084–2090.
- [141] M. Shishehbor, M.R. Pouranian, M.G. Ramezani, Molecular investigations on the interactions of graphene, crude oil fractions and mineral aggregates at low, medium and high temperatures, *Pet. Sci. Technol.* 37 (7) (2019) 804–811.
- [142] Z. Du, X. Zhu, Y. Yuan, Molecular investigation on the adhesion and deformation behaviors of asphalt binder under nanoindentation, *Constr. Build. Mater.* 295 (2021) 123683.
- [143] Y. Hou, H. Zhang, J. Wu, L. Wang, H. Xiong, Study on the microscopic friction between tire and asphalt pavement based on molecular dynamics simulation, *Int. J. Pavement Res. Technol.* 11 (2018) 205–212.
- [144] L. Kong, X. Quan, W. Luo, Y. Chen, B. Yang, H. Wang, Y. Zeng, Exploration of molecular dynamics for the adsorption of anionic emulsifier on the main chemical composition surface of aggregate, *Constr. Build. Mater.* 292 (2021) 123210.